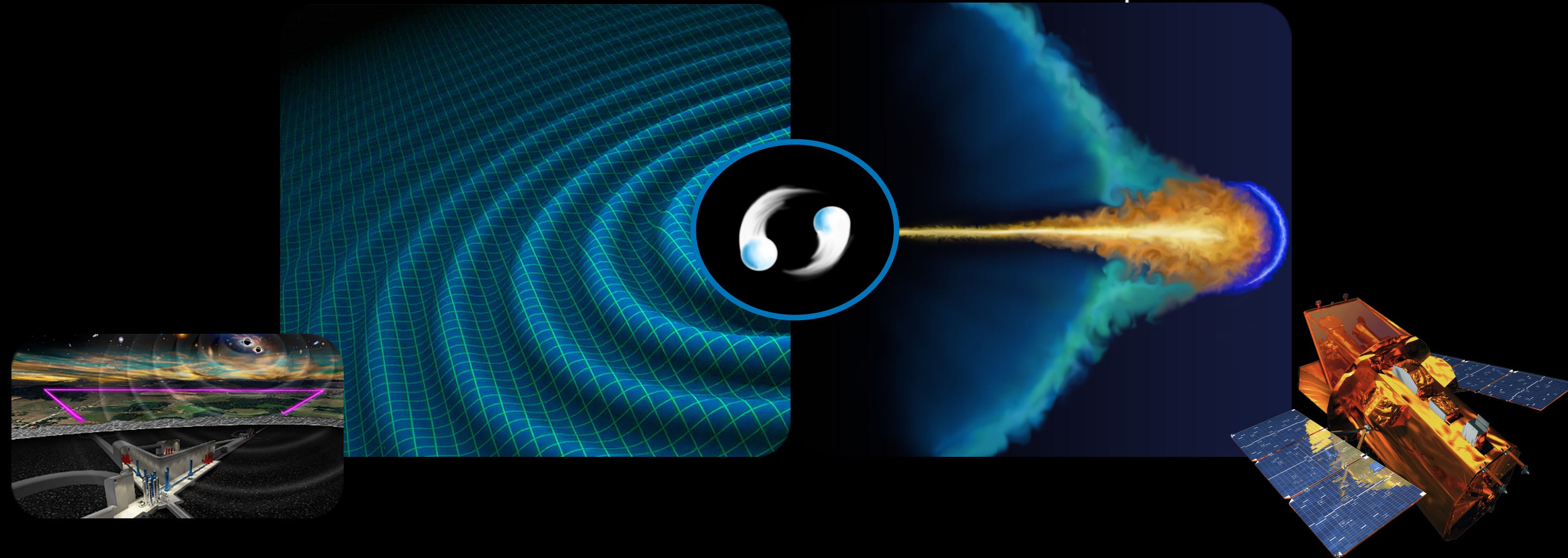
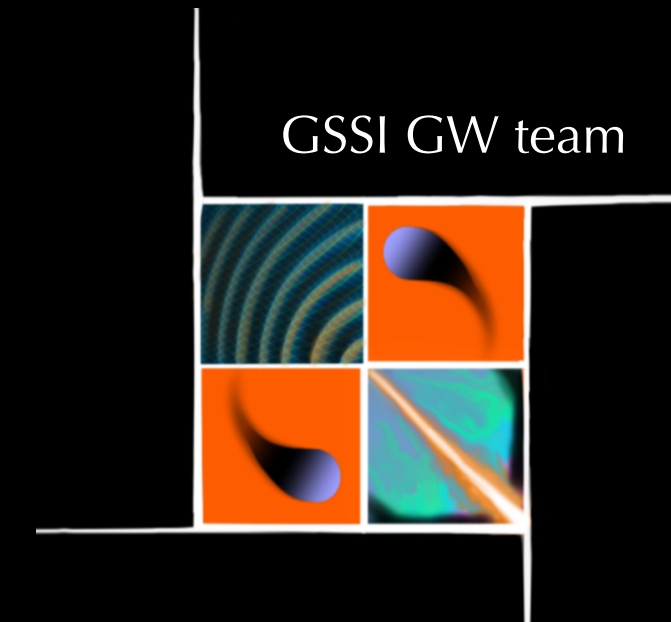


Perspectives for multi-messenger astronomy with the next generation of gravitational-wave detectors and high-energy satellites

S. Ronchini, M. Branchesi, G. Oganessian, B. Banerjee, U. Dupletsa, G. Ghirlanda, J. Harms, M. Mapelli, F. Santoliquido



Ronchini et al. 2022, doi.org/10.1051/0004-6361/202243705

We acknowledge the INFN Computing Center of Turin for computational resources

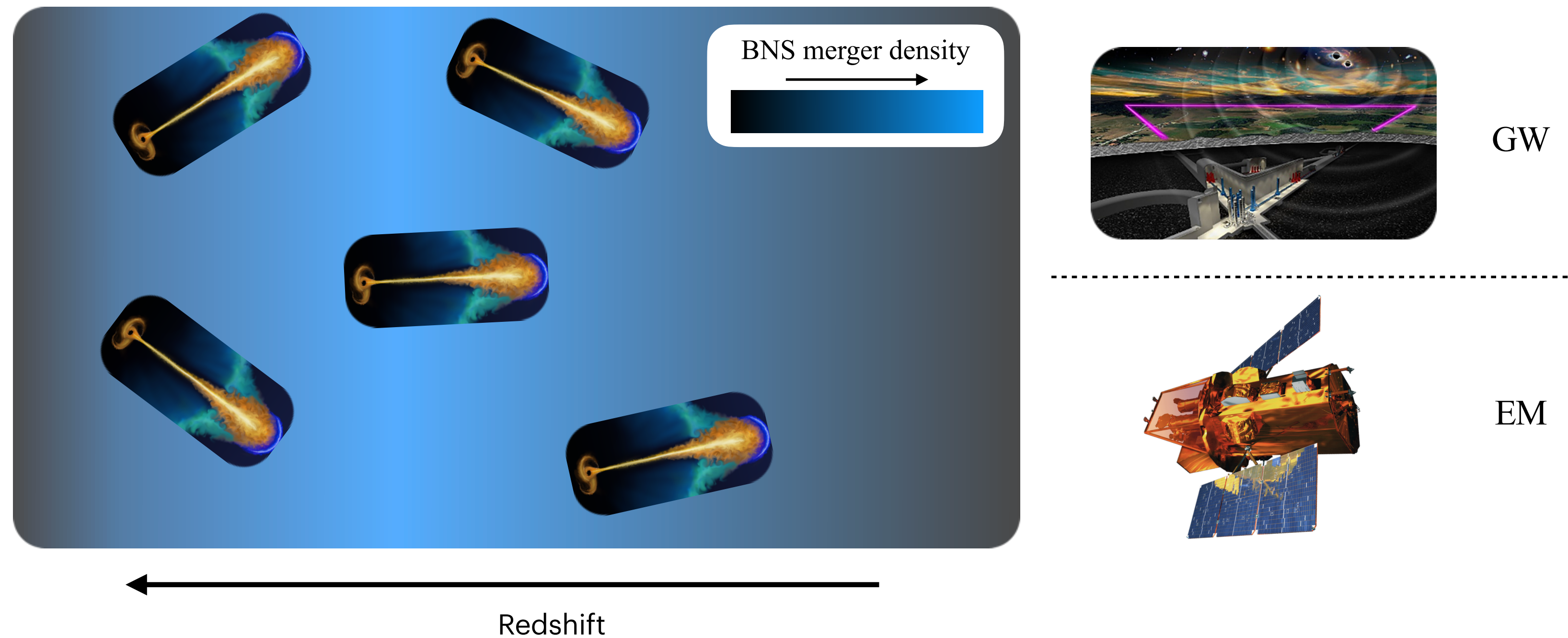
Overview

Goal of this presentation:

Provide an exhaustive view about the **joint detection** of:

1. **gravitational waves (GWs)**

2. Electromagnetic counterpart in the **high energy domain**
from the coalescence of **binary NS**, in the era of **3G GW detectors**



Points on which I will focus:

- Role of **wide field instruments** for the identification of the EM counterpart
- **GW sky localisation**
- For the follow-up, define a strategy to **prioritise the GW sources** with highest probability to have detectable EM emission
- Role of **sensitive telescopes** to characterise the multi-wavelength emission

Method: from BNS mergers to short GRBs

Redshift distribution of BNS mergers from population synthesis model

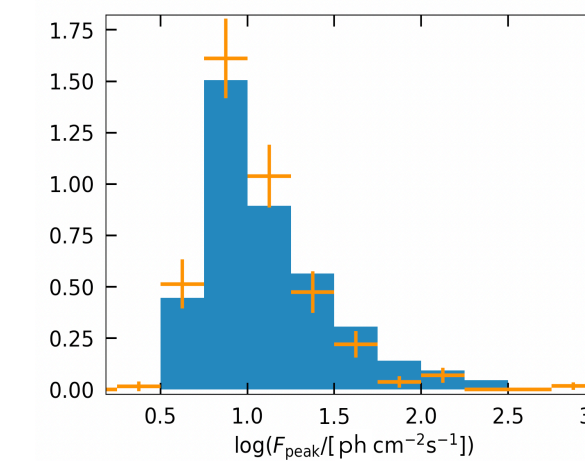
Phenomenological model for prompt emission

Estimate of the prompt and afterglow emission, assuming the same jet structure derived for GW 170817

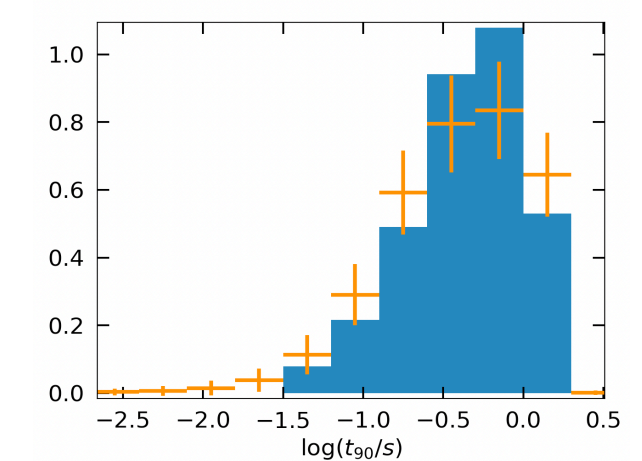
Comparison with properties of Fermi-GBM sample

Reliable predictions for future high-energy satellites

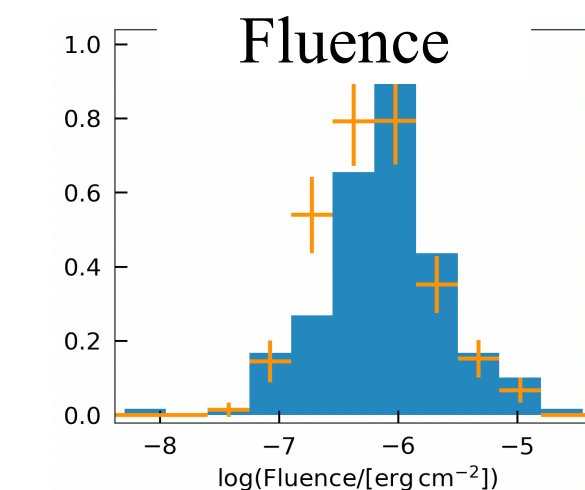
Peak flux



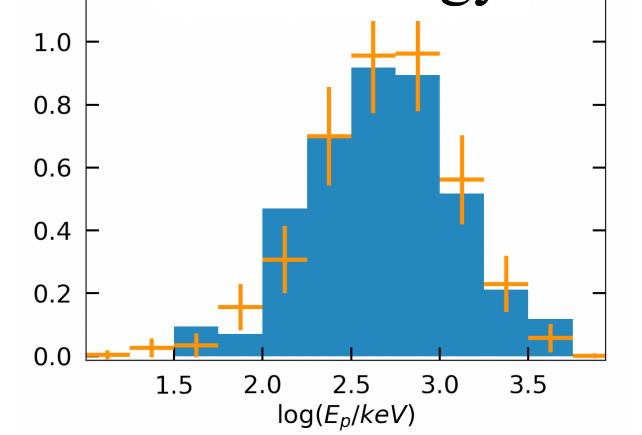
Burst duration



Fluence

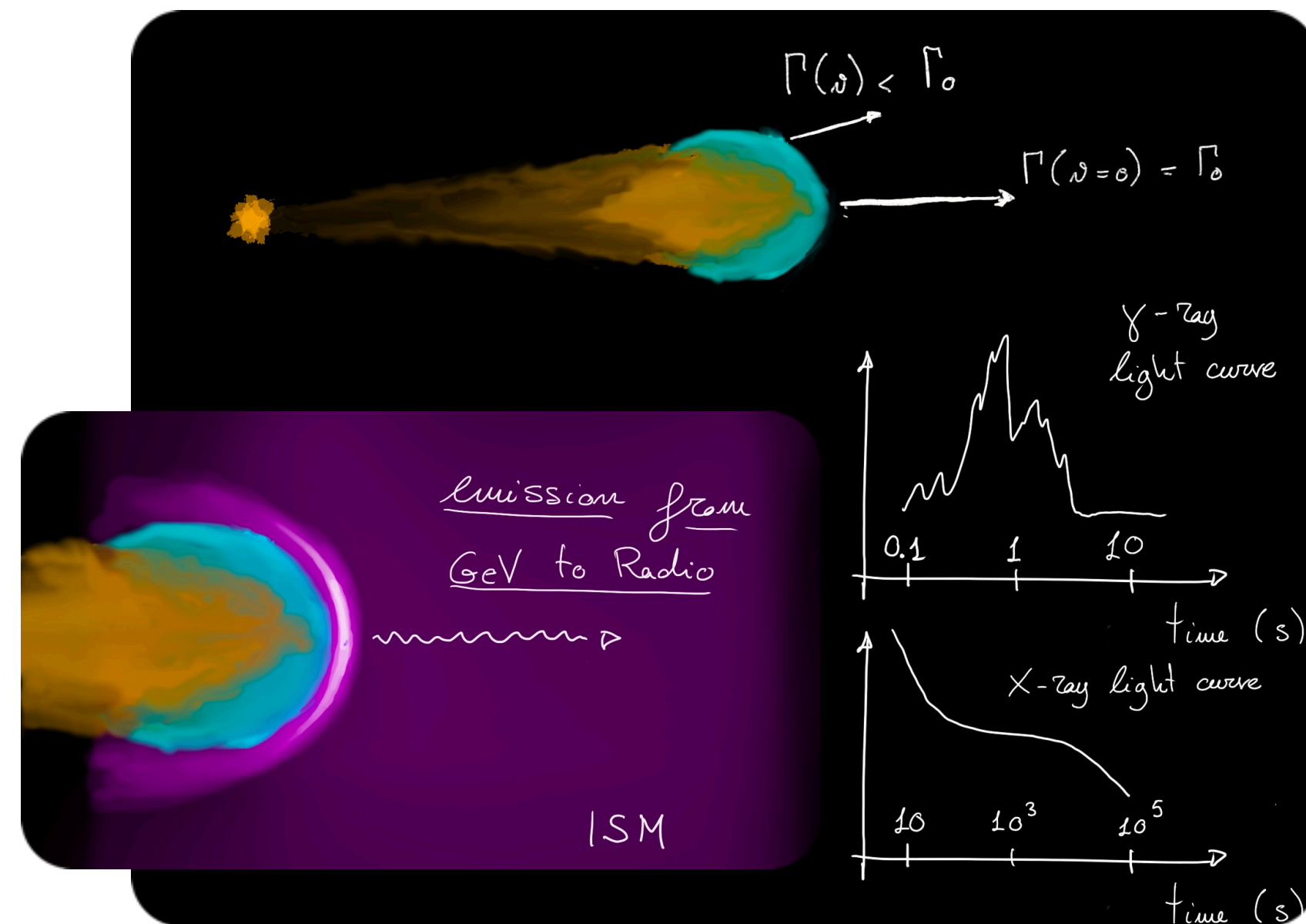


Peak energy

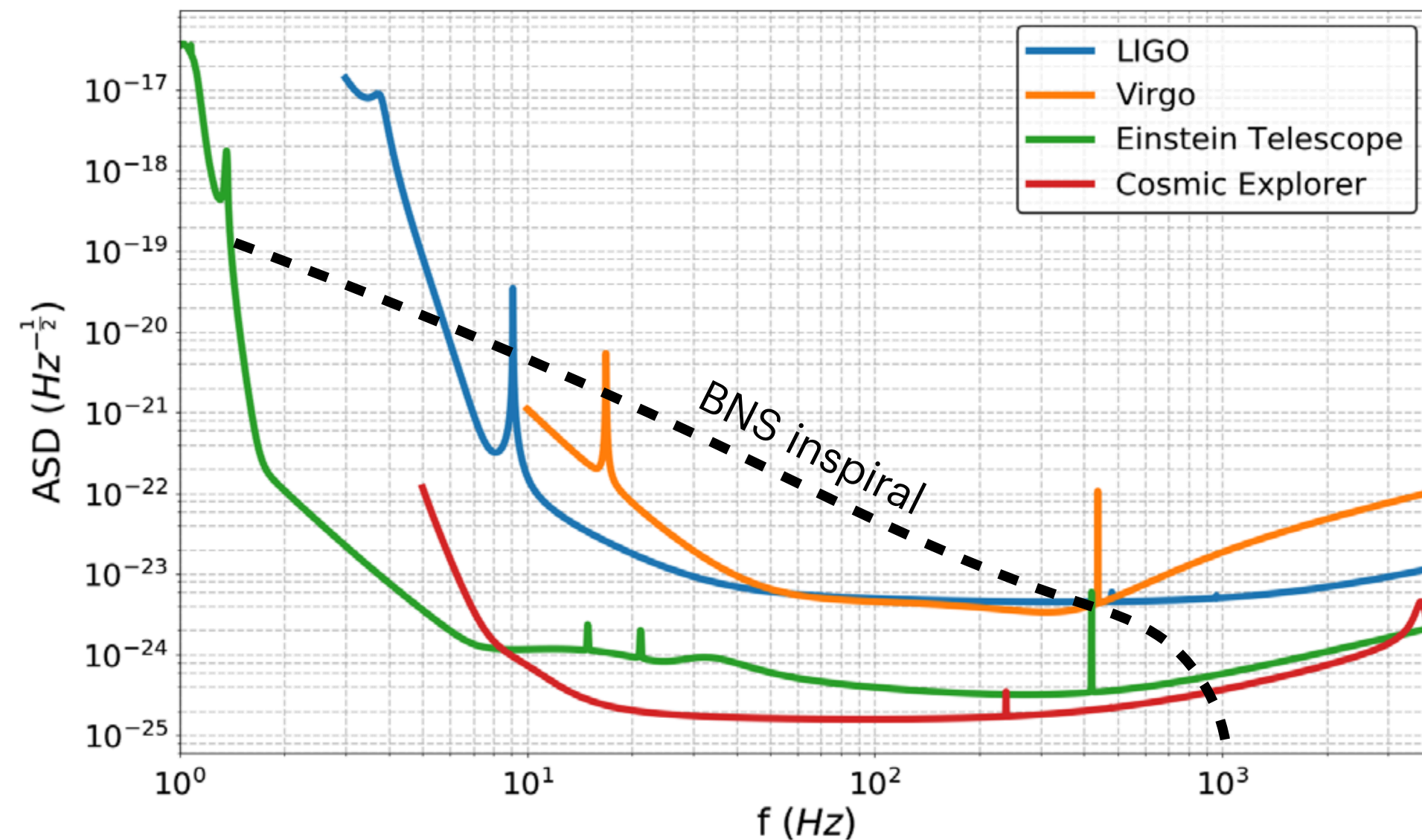


+

Fermi-GBM rate of short GRBs

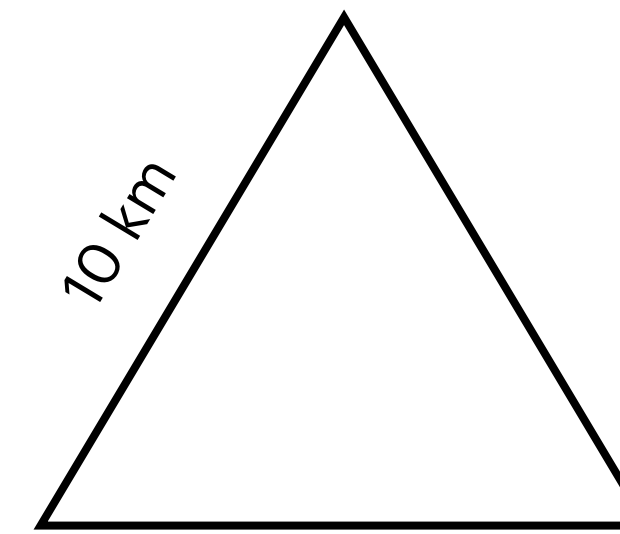


The 3rd generation of GW detectors

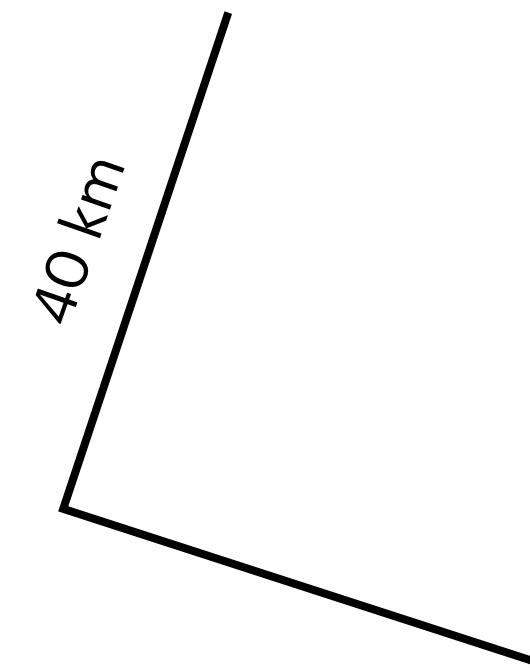


From Chan et al. 2018

1. Unprecedented sensitivity which allows to **have access to a yet unexplored region of the Universe**, beyond the star formation peak time
2. Possibility to **probe the early inspiral phase**, relevant for a good estimation of the sky localisation, thanks to the exploitation of Earth rotation



Einstein Telescope (ET)



Cosmic Explorer (CE)

GW Parameter estimation



GWFISH

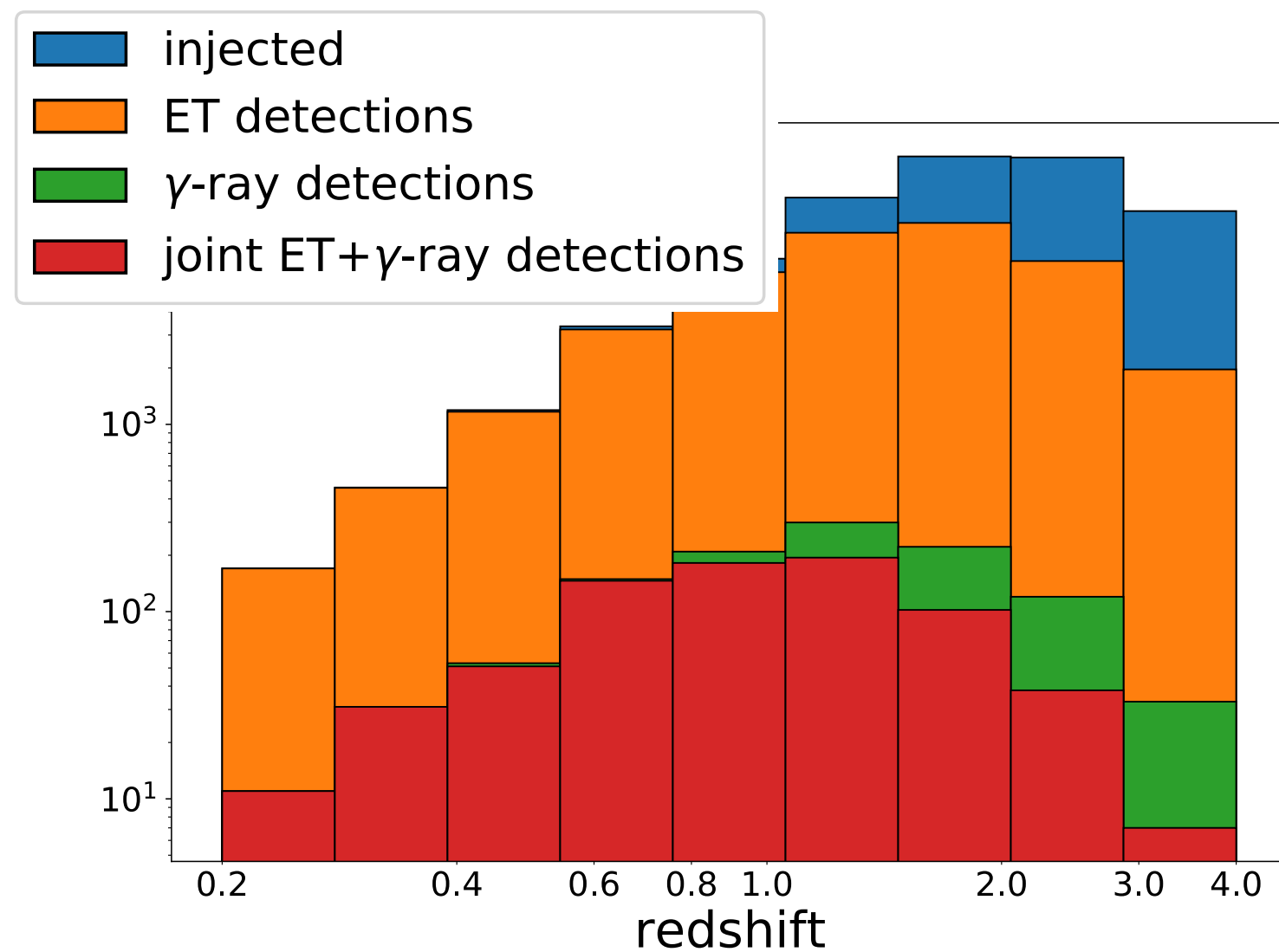
Harms et al. 2022
arXiv:2205.02499

- Based on **Fisher matrix** approximation
- **Fast** and computationally efficient

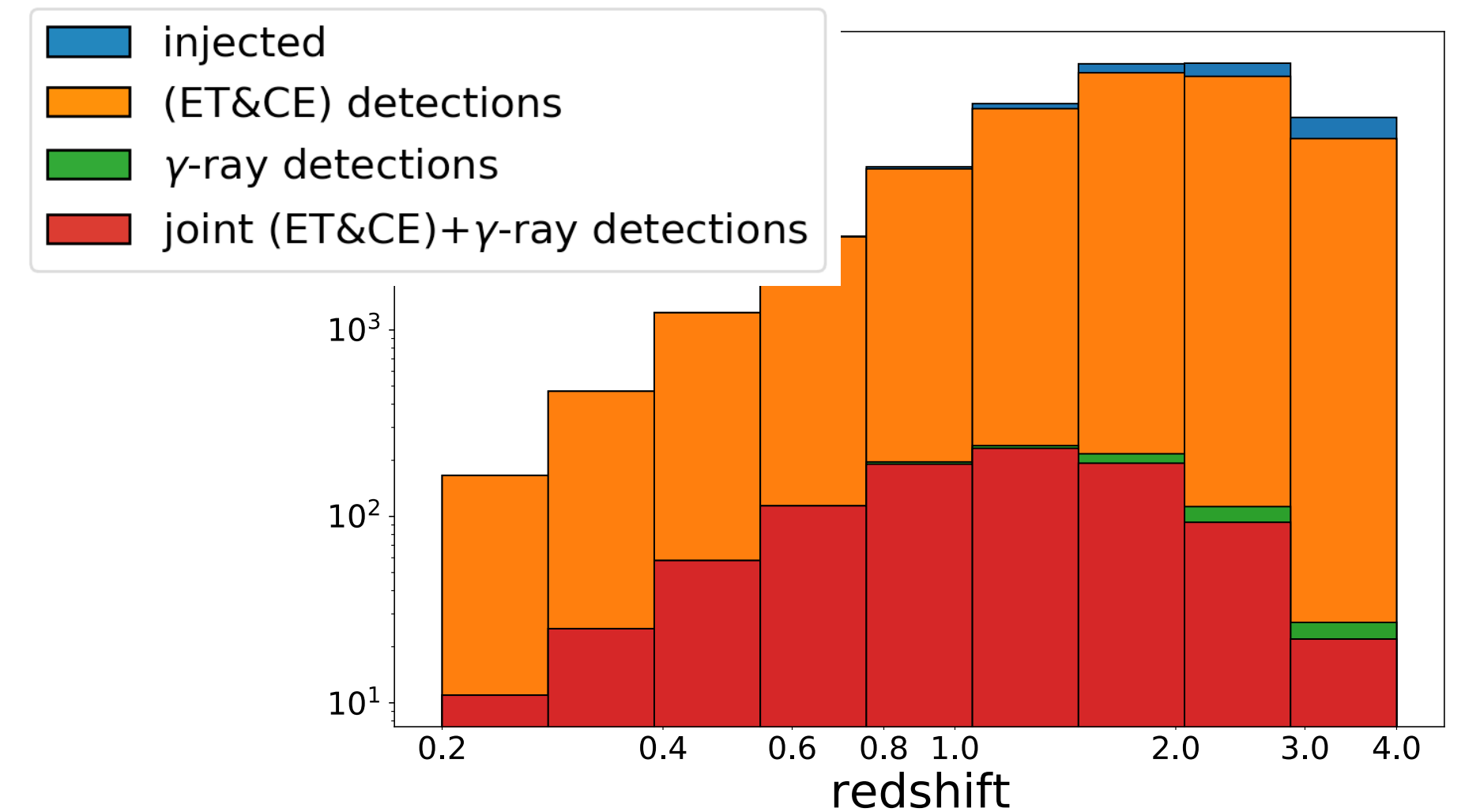
Joint detection of γ -ray emission and GWs

INSTRUMENT	band MeV	F_{lim} erg cm $^{-2}$ s $^{-1}$	FOV/ 4π	loc. acc.	Joint ET + γ -ray	N_{JD}/N_{γ}	Joint (ET+CE) + γ -ray	N_{JD}/N_{γ}
<i>Fermi</i> -GBM	0.01 - 25	0.5(*)	0.75	5 deg (^a)	33 $^{+14}_{-11}$	68 $^{+13}_{-18}\%$	47 $^{+14}_{-14}$	95 $^{+5}_{-7}\%$
<i>Swift</i> -BAT	0.015 - 0.15	2×10^{-8}	0.11	1-3 arcmin	10 $^{+3}_{-3}$	62 $^{+11}_{-14}\%$	13 $^{+5}_{-4}$	94 $^{+6}_{-7}\%$
SVOM-ECLAIRs	0.004 - 0.250	1.792(*)	0.16	< 10 arcmin	3 $^{+1}_{-1}$	69 $^{+10}_{-9}\%$	4 $^{+1}_{-1}$	95 $^{+5}_{-4}\%$
SVOM-GRM	0.03 - 5	0.23(*)	0.16	\sim 5 deg	9 $^{+4}_{-3}$	59 $^{+6}_{-6}\%$	14 $^{+6}_{-4}$	92 $^{+3}_{-3}\%$
THESEUS-XGIS	0.002 - 10	3×10^{-8}	0.16	< 15 arcmin	10 $^{+5}_{-4}$	63 $^{+13}_{-13}\%$	15 $^{+6}_{-4}$	94 $^{+6}_{-7}\%$
HERMES	0.05 - 0.3	0.2(*)	1.0	1 deg	84 $^{+42}_{-30}$	61 $^{+10}_{-11}\%$	139 $^{+54}_{-36}$	94 $^{+6}_{-6}\%$
TAP-GTM	0.01 - 1	1(*)	1.0	20 deg	60 $^{+24}_{-24}$	67 $^{+13}_{-14}\%$	84 $^{+30}_{-24}$	95 $^{+5}_{-6}\%$

Fermi GBM+ET



Fermi GBM+(ET&CE)

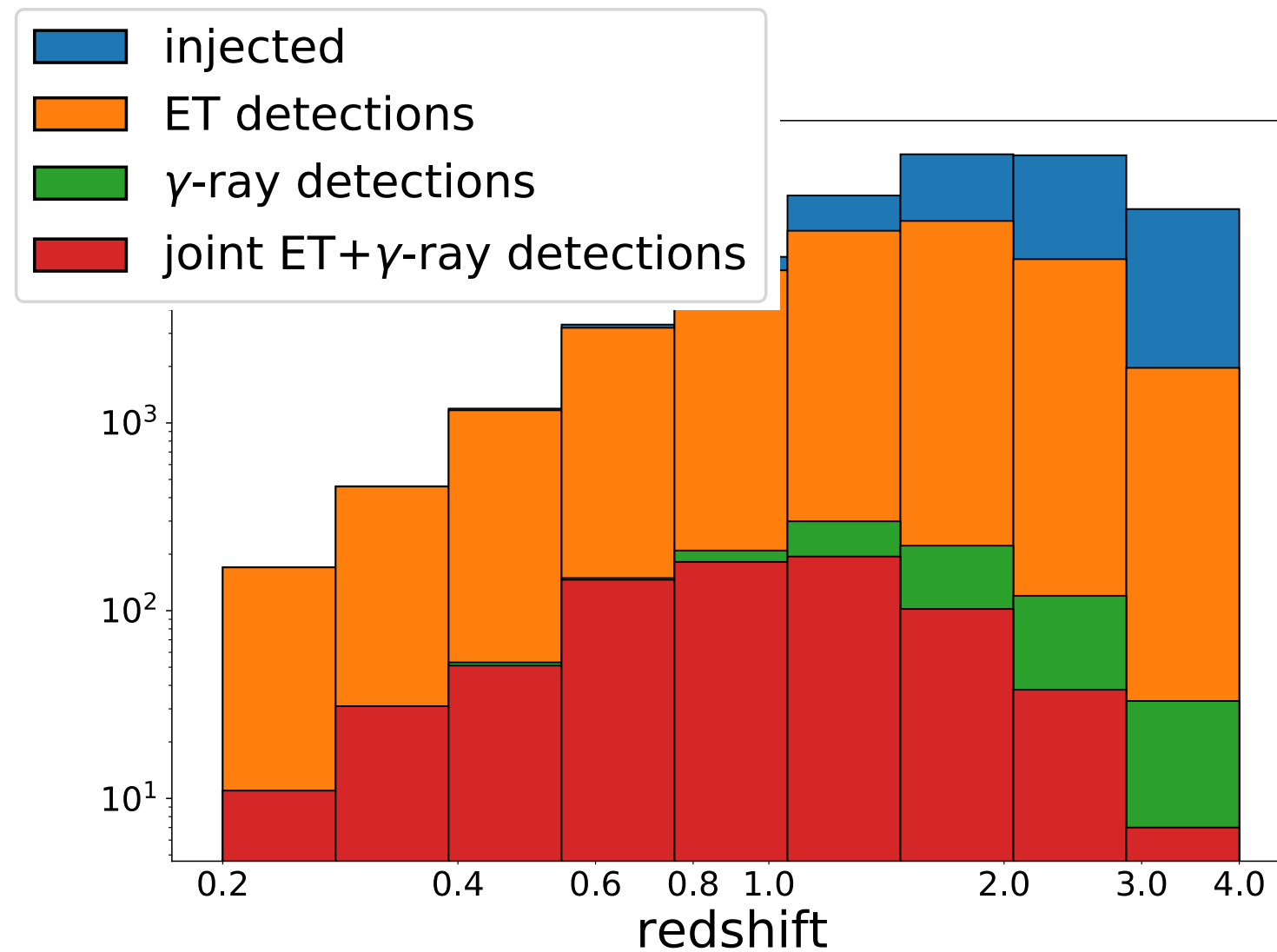


Joint detection of γ -ray emission and GWs

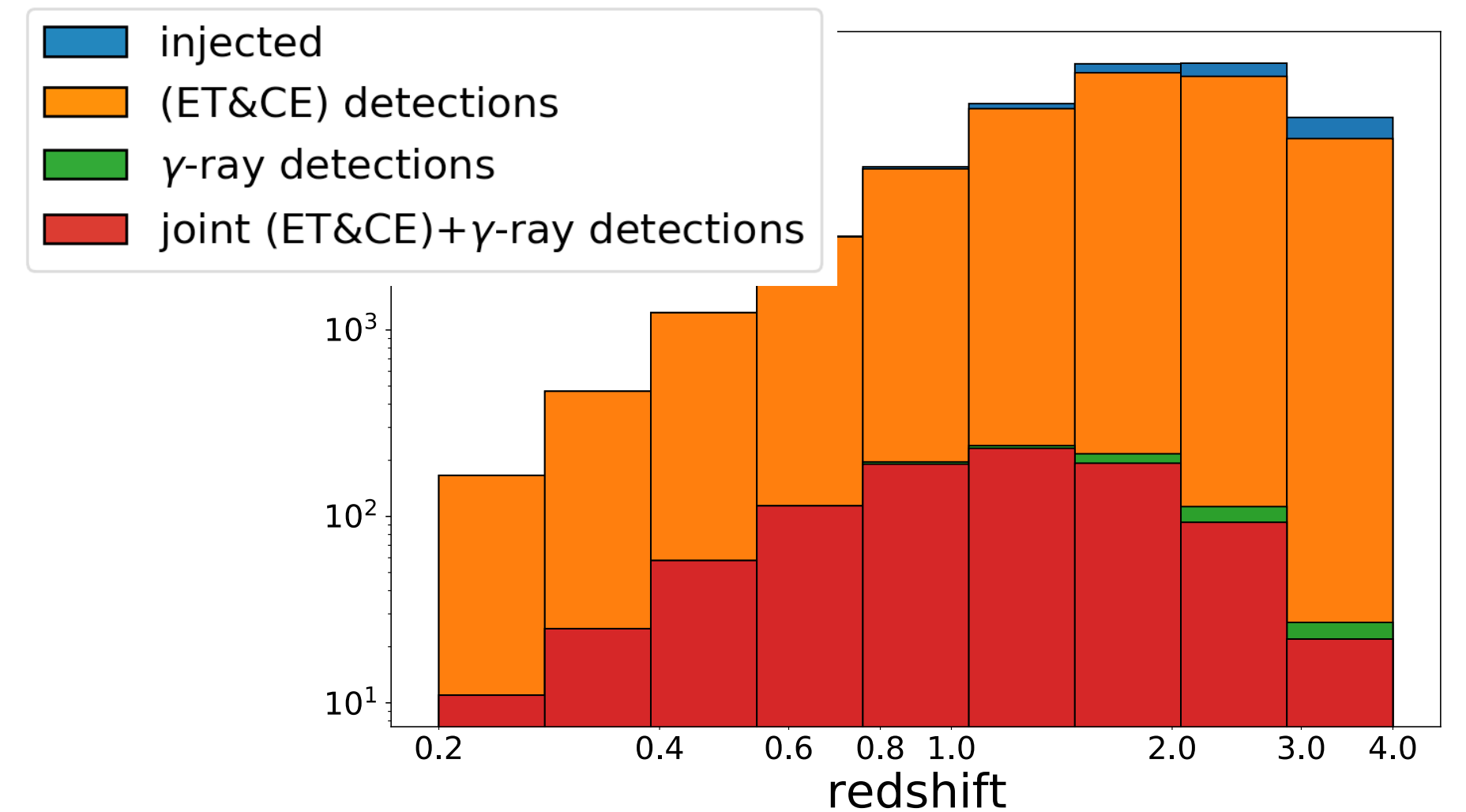
INSTRUMENT	band MeV	F_{lim} $\text{erg cm}^{-2} \text{s}^{-1}$	FOV/ 4π	loc. acc.	Joint ET + γ -ray	N_{JD}/N_γ	Joint (ET+CE) + γ -ray	N_{JD}/N_γ
<i>Fermi</i> -GBM	0.01 - 25	0.5(*)	0.75	5 deg (^a)	33^{+14}_{-11}	$68^{+13}_{-18}\%$	47^{+14}_{-14}	$95^{+5}_{-7}\%$
<i>Swift</i> -BAT	0.015 - 0.15	2×10^{-8}	0.11	1-3 arcmin	10^{+3}_{-3}	$62^{+11}_{-14}\%$	13^{+5}_{-4}	$94^{+6}_{-7}\%$
SVOM-ECLAIRs	0.004 - 0.250	1.792(*)	0.16	< 10 arcmin	3^{+1}_{-1}	$69^{+10}_{-9}\%$	4^{+1}_{-1}	$95^{+5}_{-4}\%$
SVOM-GRM	0.03 - 5	0.23(*)	0.16	~ 5 deg	9^{+4}_{-3}	$59^{+6}_{-6}\%$	14^{+6}_{-4}	$92^{+3}_{-3}\%$
THESEUS-XGIS	0.002 - 10	3×10^{-8}	0.16	< 15 arcmin	10^{+5}_{-4}	$63^{+13}_{-13}\%$	15^{+6}_{-4}	$94^{+6}_{-7}\%$
HERMES	0.05 - 0.3	0.2(*)	1.0	1 deg	84^{+42}_{-30}	$61^{+10}_{-11}\%$	139^{+54}_{-36}	$94^{+6}_{-6}\%$
TAP-GTM	0.01 - 1	1(*)	1.0	20 deg	60^{+24}_{-24}	$67^{+13}_{-14}\%$	84^{+30}_{-24}	$95^{+5}_{-6}\%$

Few but **well localised** events

Fermi GBM+ET



Fermi GBM+(ET&CE)

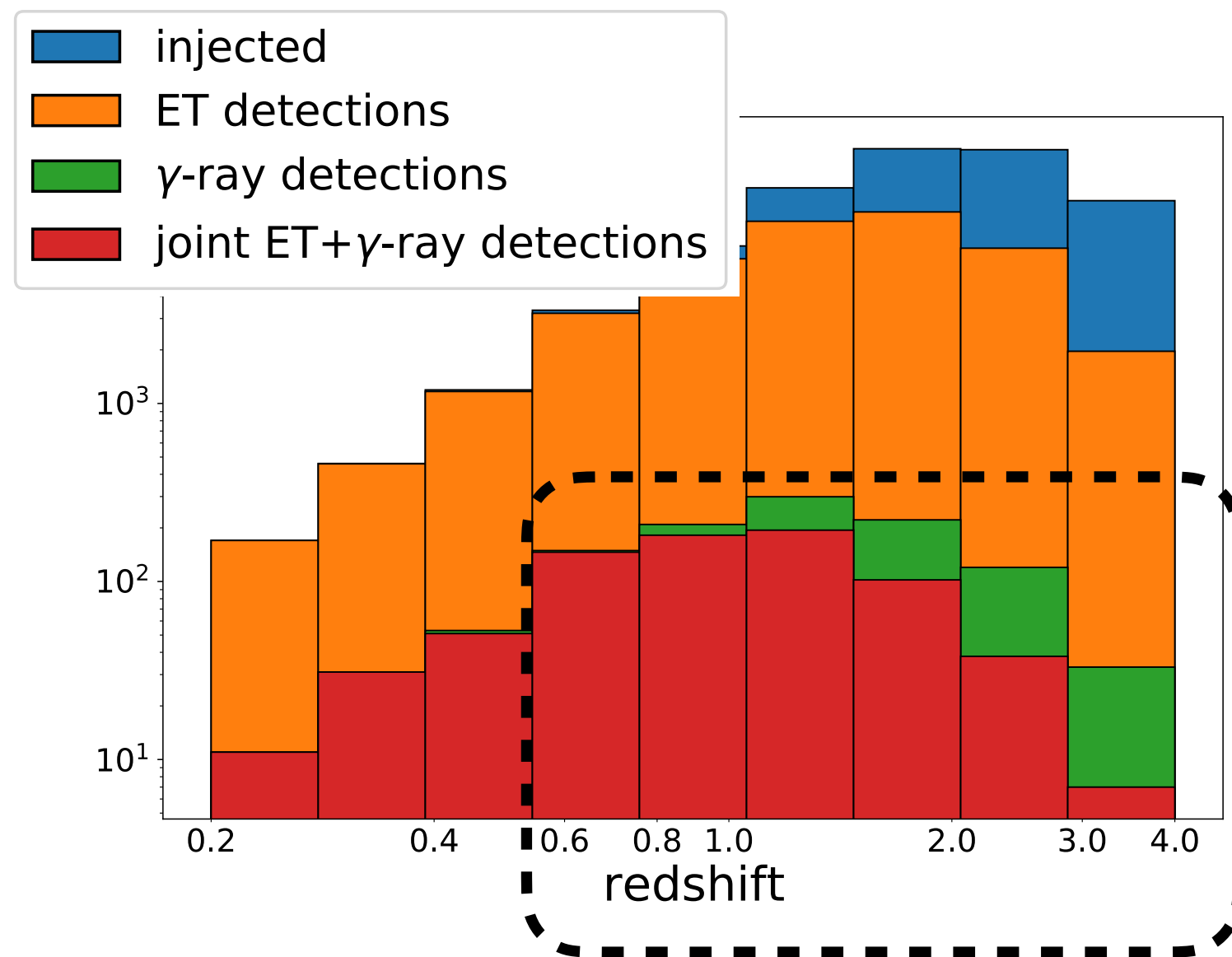


Joint detection of γ -ray emission and GWs

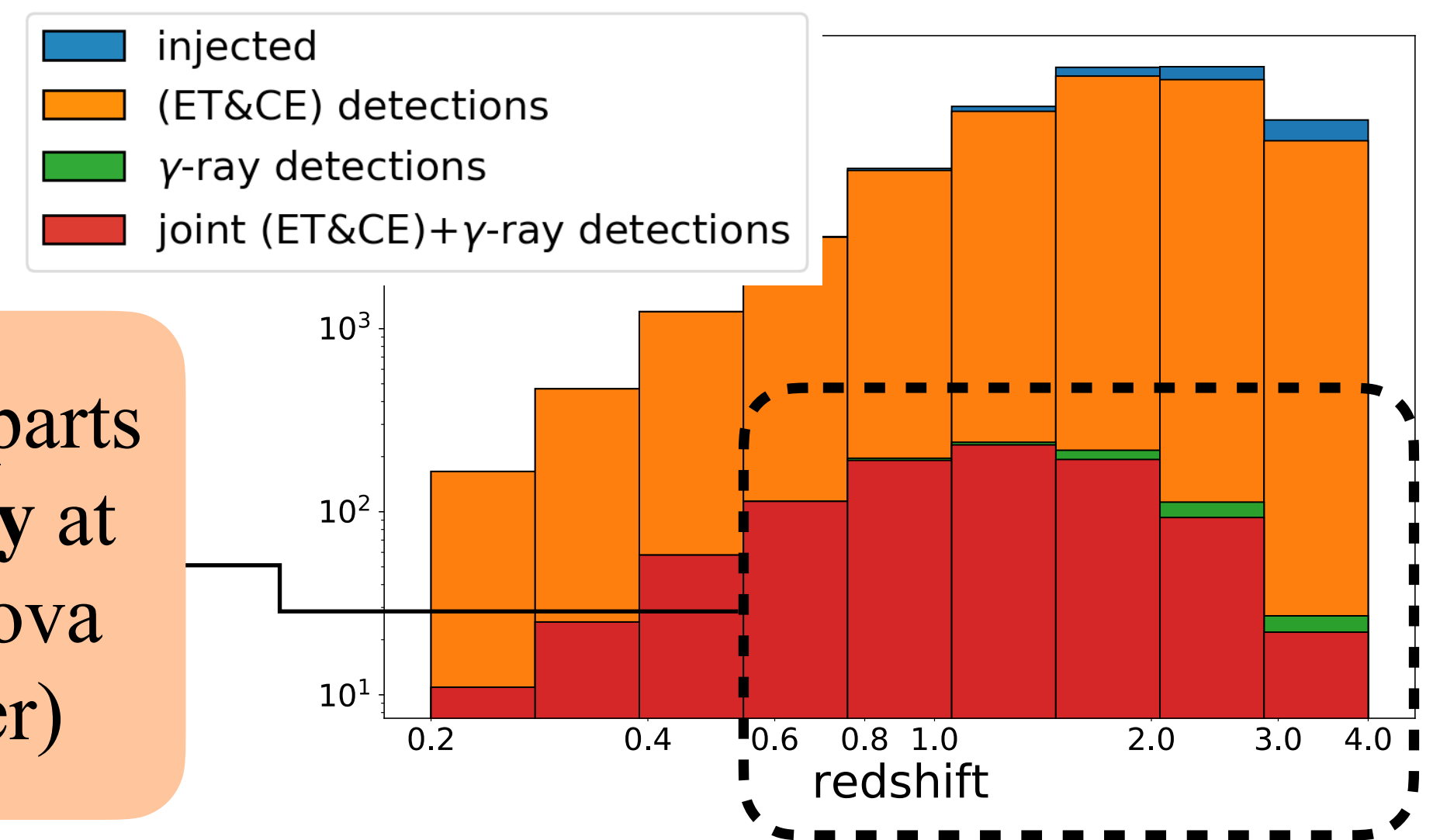
INSTRUMENT	band MeV	F_{lim} $\text{erg cm}^{-2} \text{s}^{-1}$	FOV/ 4π	loc. acc.	Joint ET + γ -ray	N_{JD}/N_γ	Joint (ET+CE) + γ -ray	N_{JD}/N_γ
<i>Fermi</i> -GBM	0.01 - 25	0.5(*)	0.75	5 deg (^a)	33^{+14}_{-11}	$68^{+13}_{-18}\%$	47^{+14}_{-14}	$95^{+5}_{-7}\%$
<i>Swift</i> -BAT	0.015 - 0.15	2×10^{-8}	0.11	1-3 arcmin	10^{+3}_{-3}	$62^{+11}_{-14}\%$	13^{+5}_{-4}	$94^{+6}_{-7}\%$
SVOM-ECLAIRs	0.004 - 0.250	1.792(*)	0.16	< 10 arcmin	3^{+1}_{-1}	$69^{+10}_{-9}\%$	4^{+1}_{-1}	$95^{+5}_{-4}\%$
SVOM-GRM	0.03 - 5	0.23(*)	0.16	~ 5 deg	9^{+4}_{-3}	$59^{+6}_{-6}\%$	14^{+6}_{-4}	$92^{+3}_{-3}\%$
THESEUS-XGIS	0.002 - 10	3×10^{-8}	0.16	< 15 arcmin	10^{+5}_{-4}	$63^{+13}_{-13}\%$	15^{+6}_{-4}	$94^{+6}_{-7}\%$
HERMES	0.05 - 0.3	0.2(*)	1.0	1 deg	84^{+42}_{-30}	$61^{+10}_{-11}\%$	139^{+54}_{-36}	$94^{+6}_{-6}\%$
TAP-GTM	0.01 - 1	1(*)	1.0	20 deg	60^{+24}_{-24}	$67^{+13}_{-14}\%$	84^{+30}_{-24}	$95^{+5}_{-6}\%$

Few but **well localised** events

Fermi GBM+ET



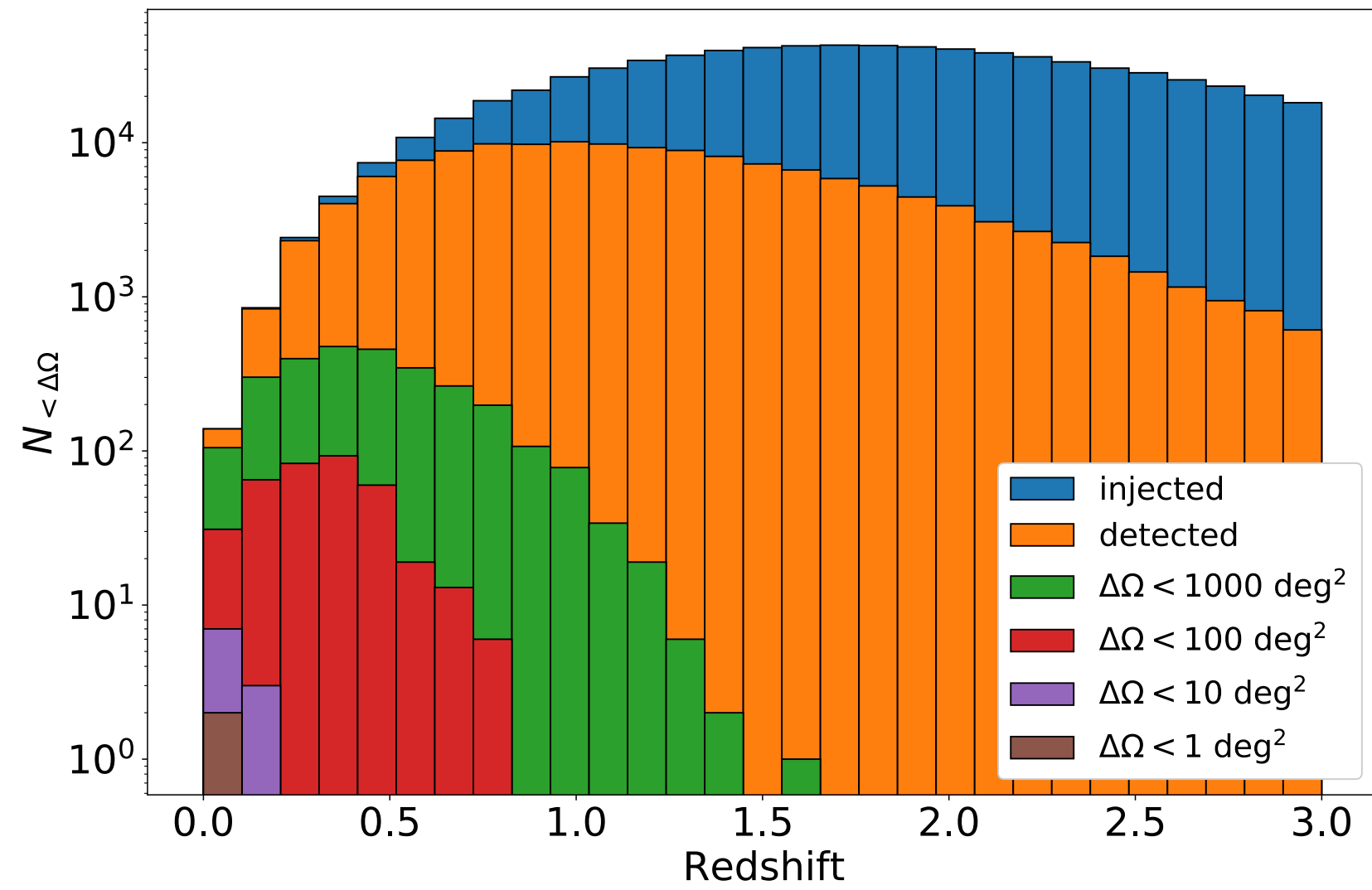
Fermi GBM+(ET&CE)



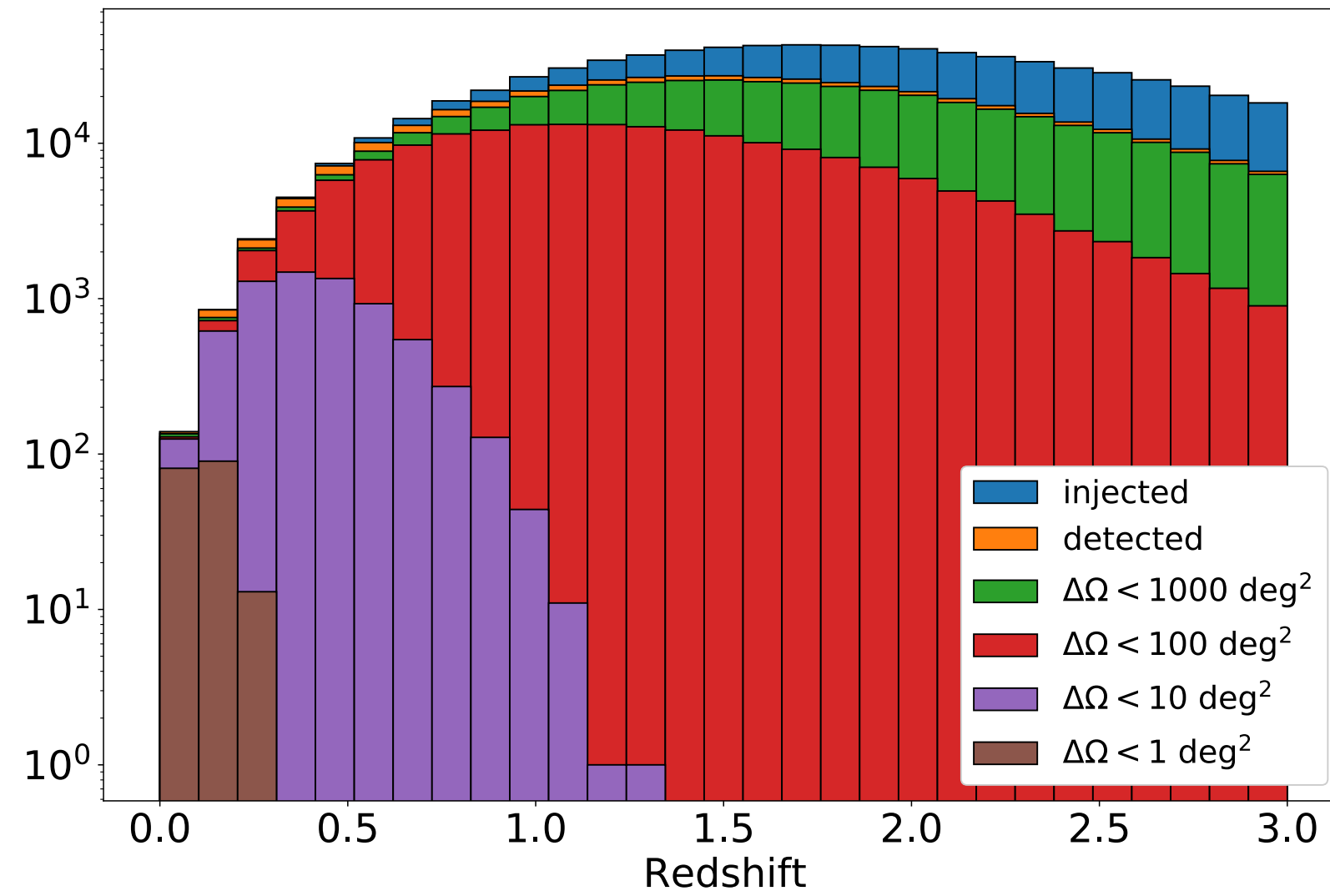
High- z GW counterparts can be detected **only** at high-energy (kilonova intrinsically fainter)

GW sky localisation

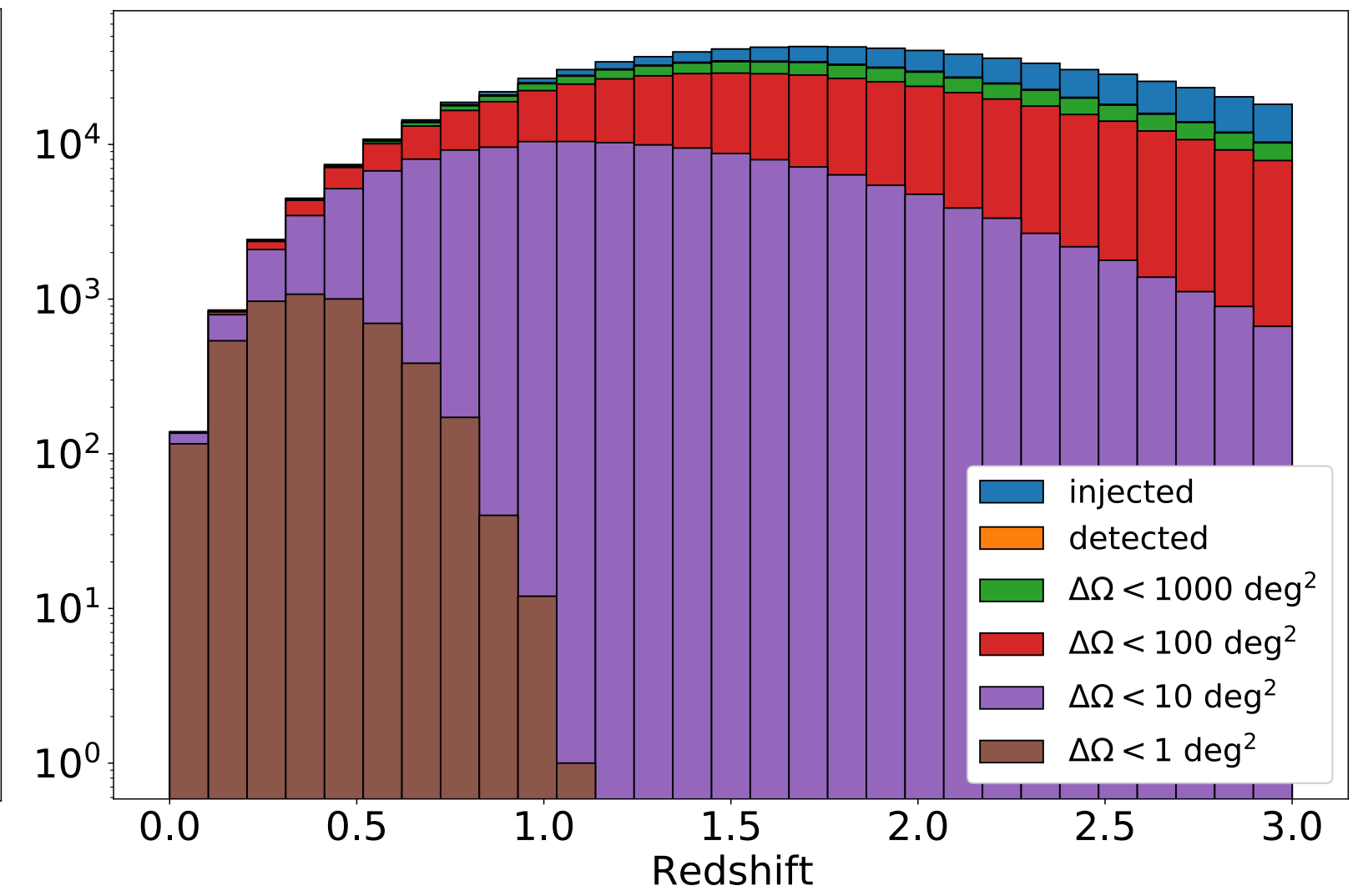
ET



ET+CE



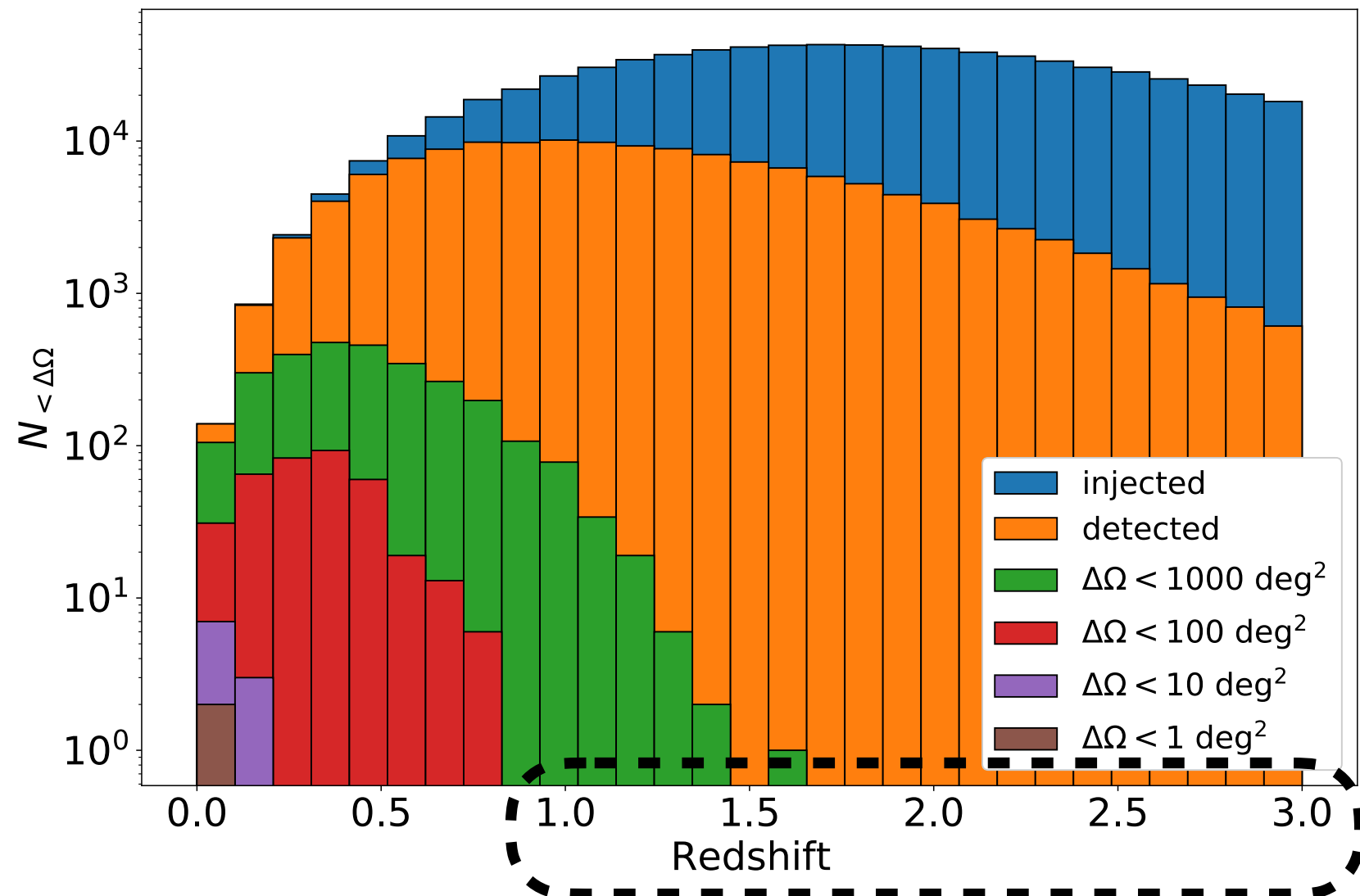
ET+2CE



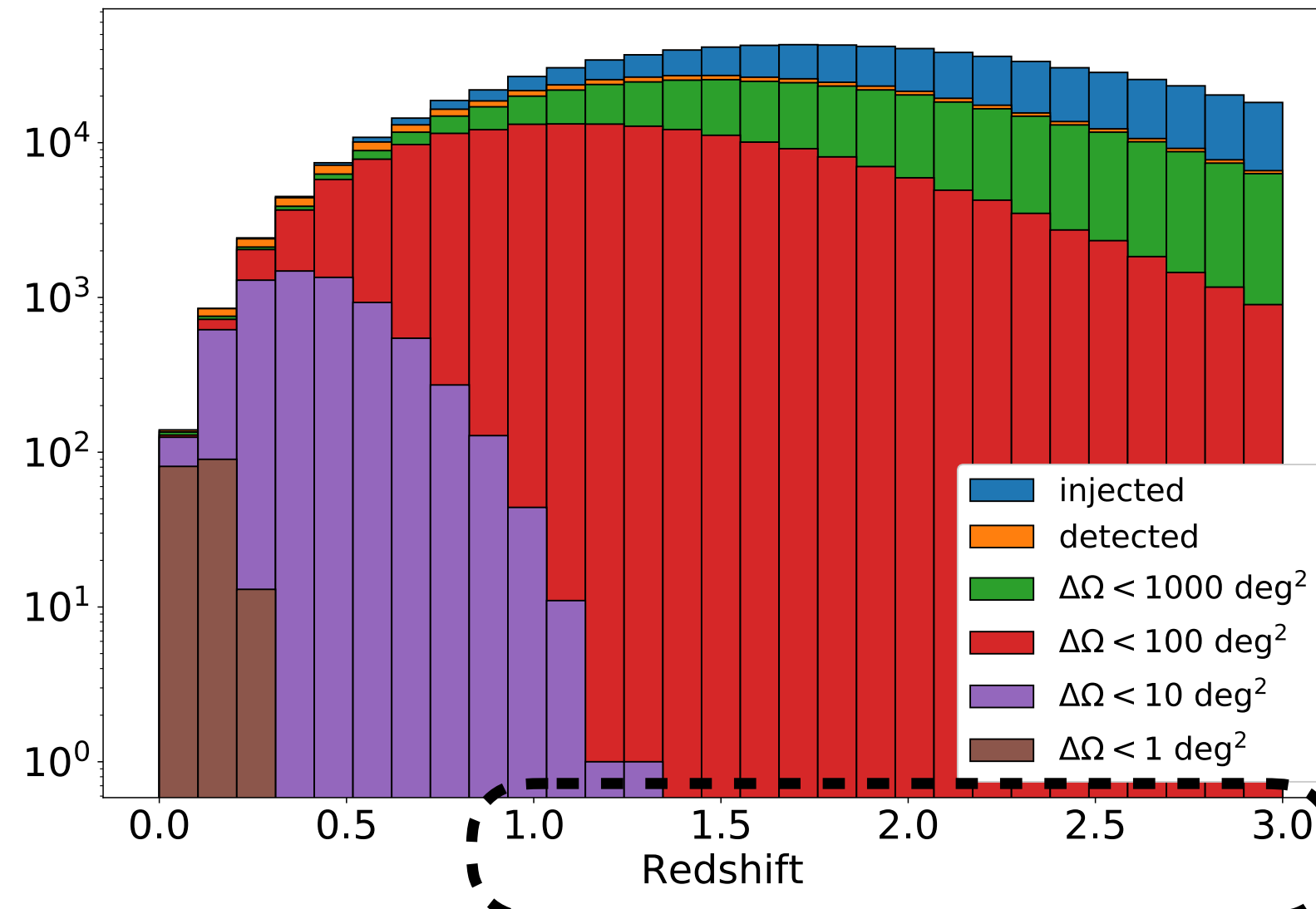
	ET	ET+CE	ET+2CE
N_{det}	143970	458801	592565
$N_{\text{det}}(\Delta\Omega < 1 \text{ deg}^2)$	2	184	5009
$N_{\text{det}}(\Delta\Omega < 10 \text{ deg}^2)$	10	6797	154167
$N_{\text{det}}(\Delta\Omega < 100 \text{ deg}^2)$	370	192468	493819
$N_{\text{det}}(\Delta\Omega < 1000 \text{ deg}^2)$	2791	428484	585317

GW sky localisation

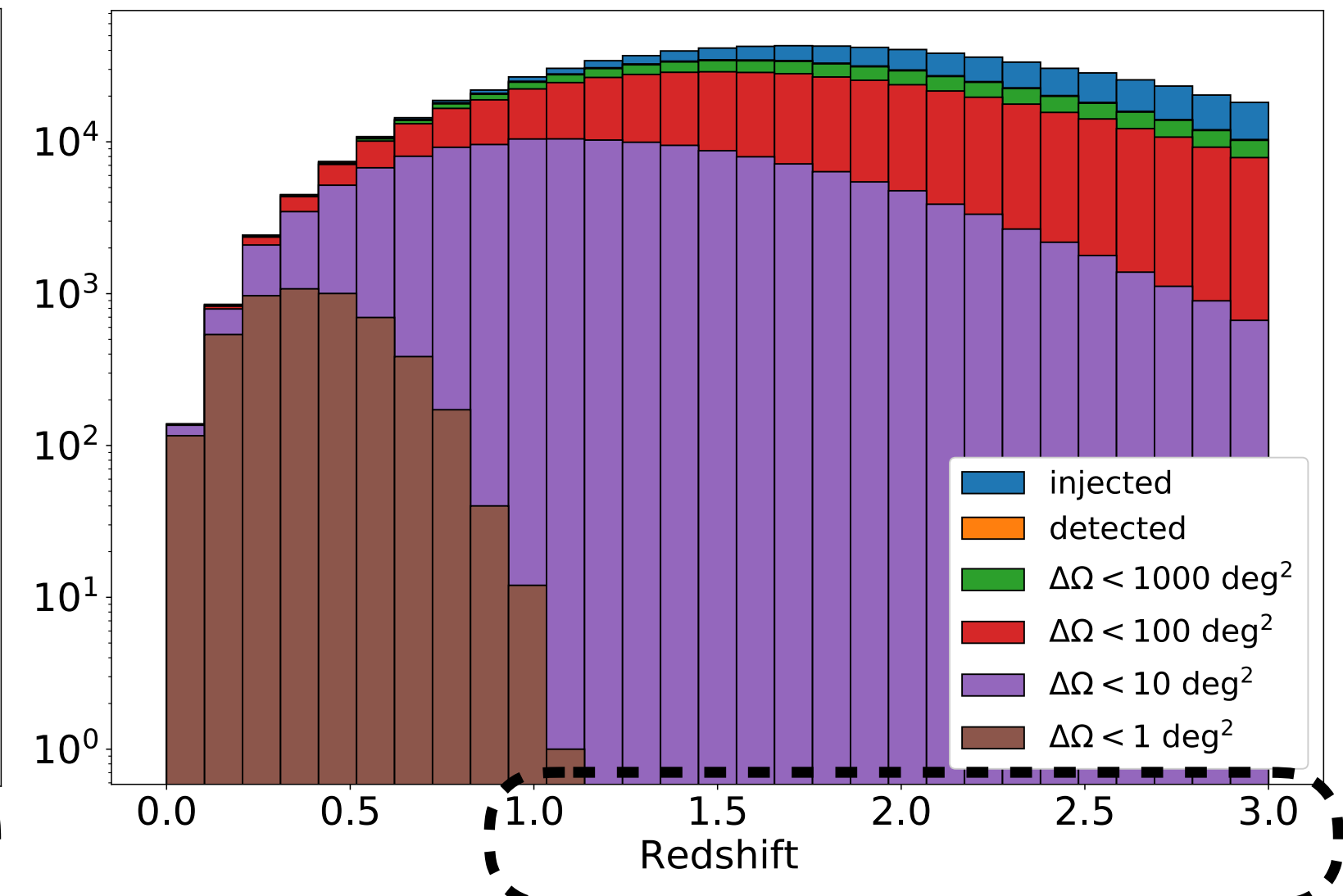
ET



ET+CE



ET+2CE



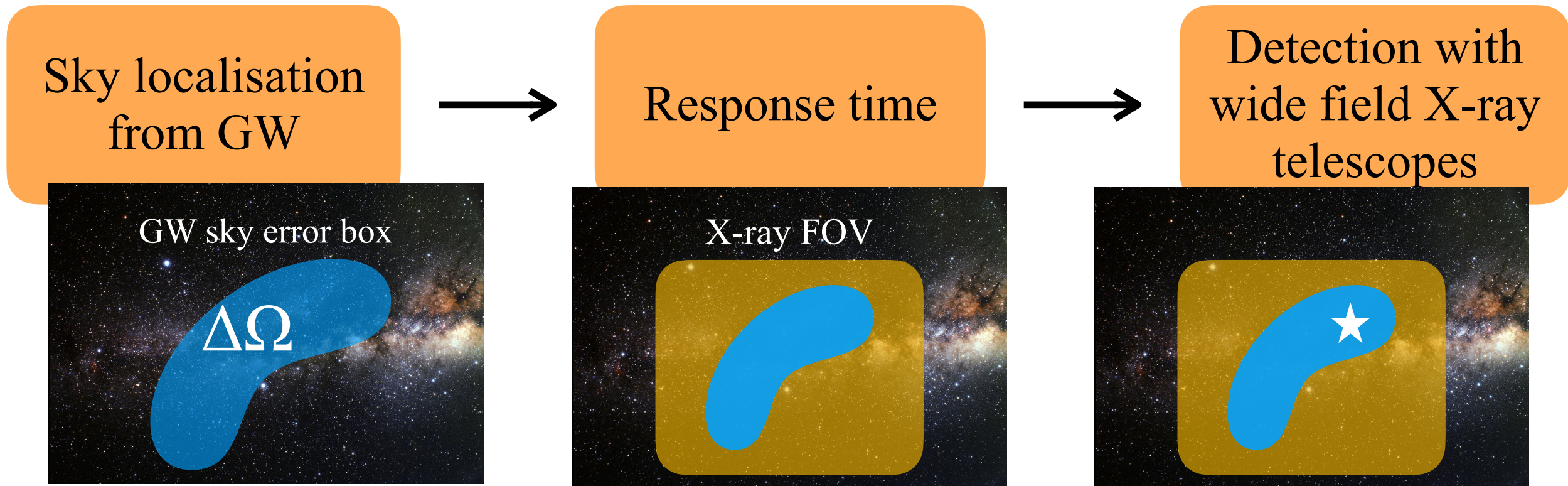
	ET	ET+CE	ET+2CE
N_{det}	143970	458801	592565
$N_{\text{det}}(\Delta\Omega < 1 \text{ deg}^2)$	2	184	5009
$N_{\text{det}}(\Delta\Omega < 10 \text{ deg}^2)$	10	6797	154167
$N_{\text{det}}(\Delta\Omega < 100 \text{ deg}^2)$	370	192468	493819
$N_{\text{det}}(\Delta\Omega < 1000 \text{ deg}^2)$	2791	428484	585317

High-z GW source localisation is given by counterparts detected by **wide field X-ray and γ -ray telescopes** with arcmin localisation capabilities

Detectability of the afterglow emission: survey vs pointing

How to detect X-ray emission:

1. In **survey mode**: probability $\sim \text{FOV}/4\pi$ of detecting by chance the source
2. In **pointing mode**: selection of the sources with $\Delta\Omega < 100 \text{ deg}^2$



	THESEUS-SXI	TAP	Einstein Probe	Gamow
Energy band	0.3-5 keV	0.3-5 keV	0.5-4 keV	0.3-5 keV
Field of view	0.5 sr	0.4 sr	1.1 sr	0.4 sr

Number of BNS mergers / yr detected in GWs and X-rays

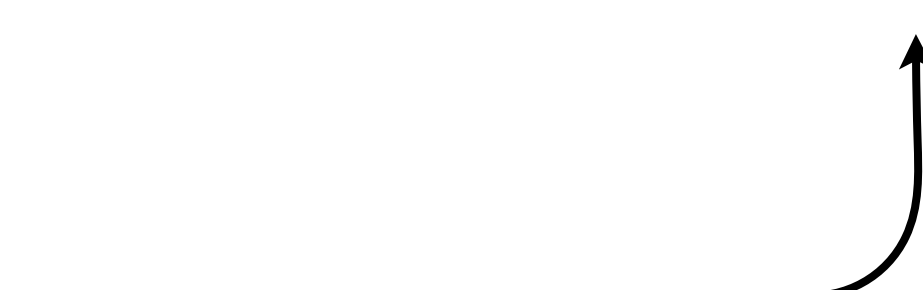
Survey mode

	ET	ET+2CE
EP	50^{+15}_{-16}	64^{+12}_{-20}
<i>Gamow</i>	9^{+2}_{-2}	10^{+3}_{-3}
THESEUS-SXI	11^{+3}_{-3}	13^{+4}_{-3}
THESEUS-(SXI+XGIS)	23^{+6}_{-5}	27^{+7}_{-5}
TAP-WFI	16^{+3}_{-4}	17^{+6}_{-3}

Pointing mode

	ET	ET+CE	ET+2CE
EP	9^{+5}_{-3}	294^{+80}_{-59}	359^{+168}_{-110}
THESEUS-SXI/ <i>Gamow</i>	7^{+5}_{-3}	95^{+43}_{-14}	122^{+41}_{-23}
TAP-WFI	8^{+5}_{-3}	182^{+43}_{-31}	225^{+76}_{-72}

For 2-3 GW detectors active,
pointing better than survey,
but...



Caveats about pointing

	ET	ET+CE	ET+2CE
EP	9^{+5}_{-3}	294^{+80}_{-59}	359^{+168}_{-110}
THESEUS-SXI/ <i>Gamow</i>	7^{+5}_{-3}	95^{+43}_{-14}	122^{+41}_{-23}
TAP-WFI	8^{+5}_{-3}	182^{+43}_{-31}	225^{+76}_{-72}



Following-up all the sources with $\Delta\Omega < 100 \text{ deg}^2$ is **unfeasible**



Other GW parameters should be exploited to restrict the selection:

- **SNR**
- **Viewing angle** and relative error
- **Luminosity distance** and relative error

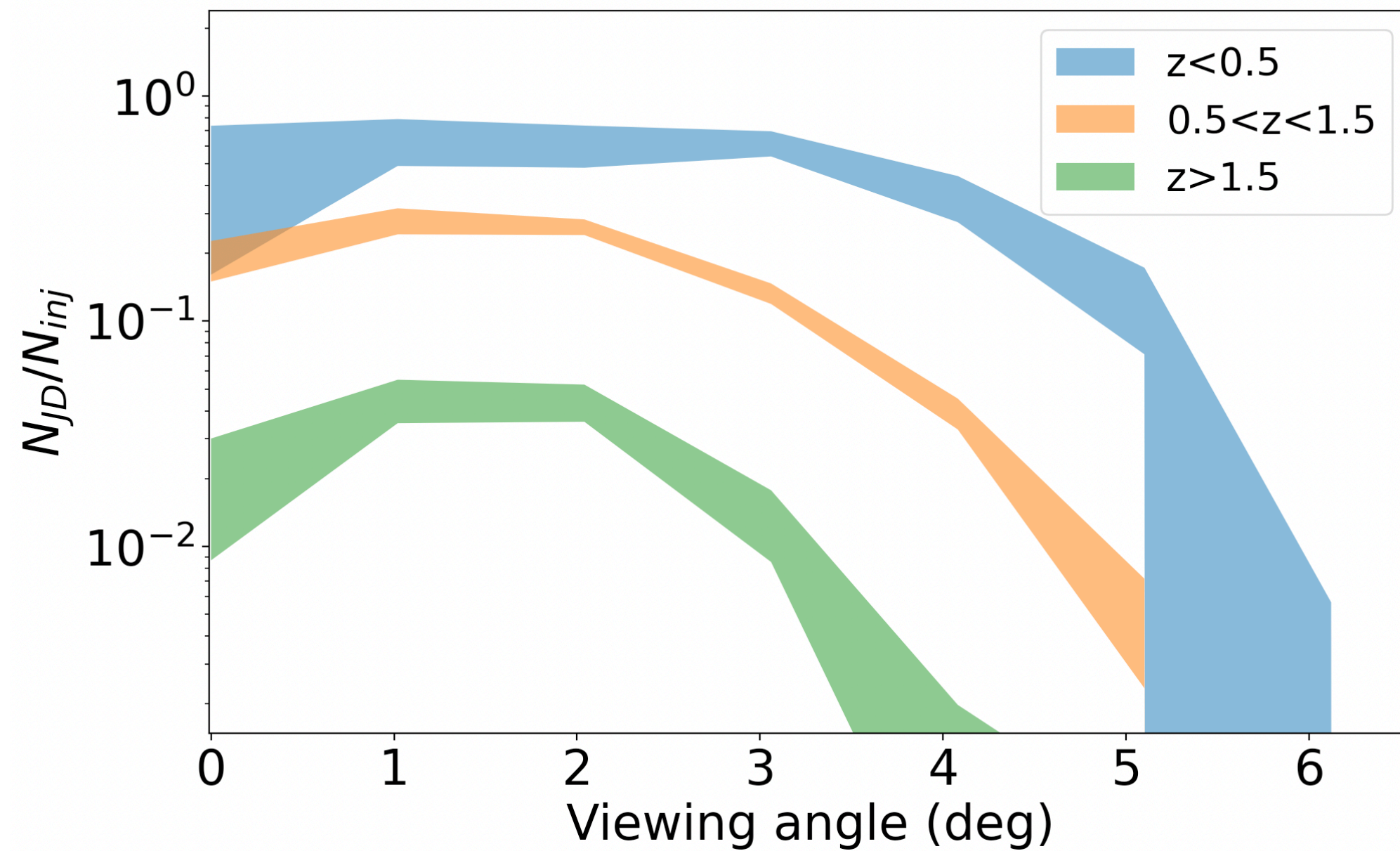
A **rapid response** is necessary to catch the brighter phase of the afterglow

	100 s	1 hr	4 hr
Einstein Probe	359^{+168}_{-110}	48^{+24}_{-15}	17^{+15}_{-10}
THESEUS-SXI/ <i>Gamow</i>	122^{+41}_{-23}	12 ± 7	< 9
TAP-WFI	225^{+76}_{-72}	50^{+20}_{-10}	17^{+10}_{-5}

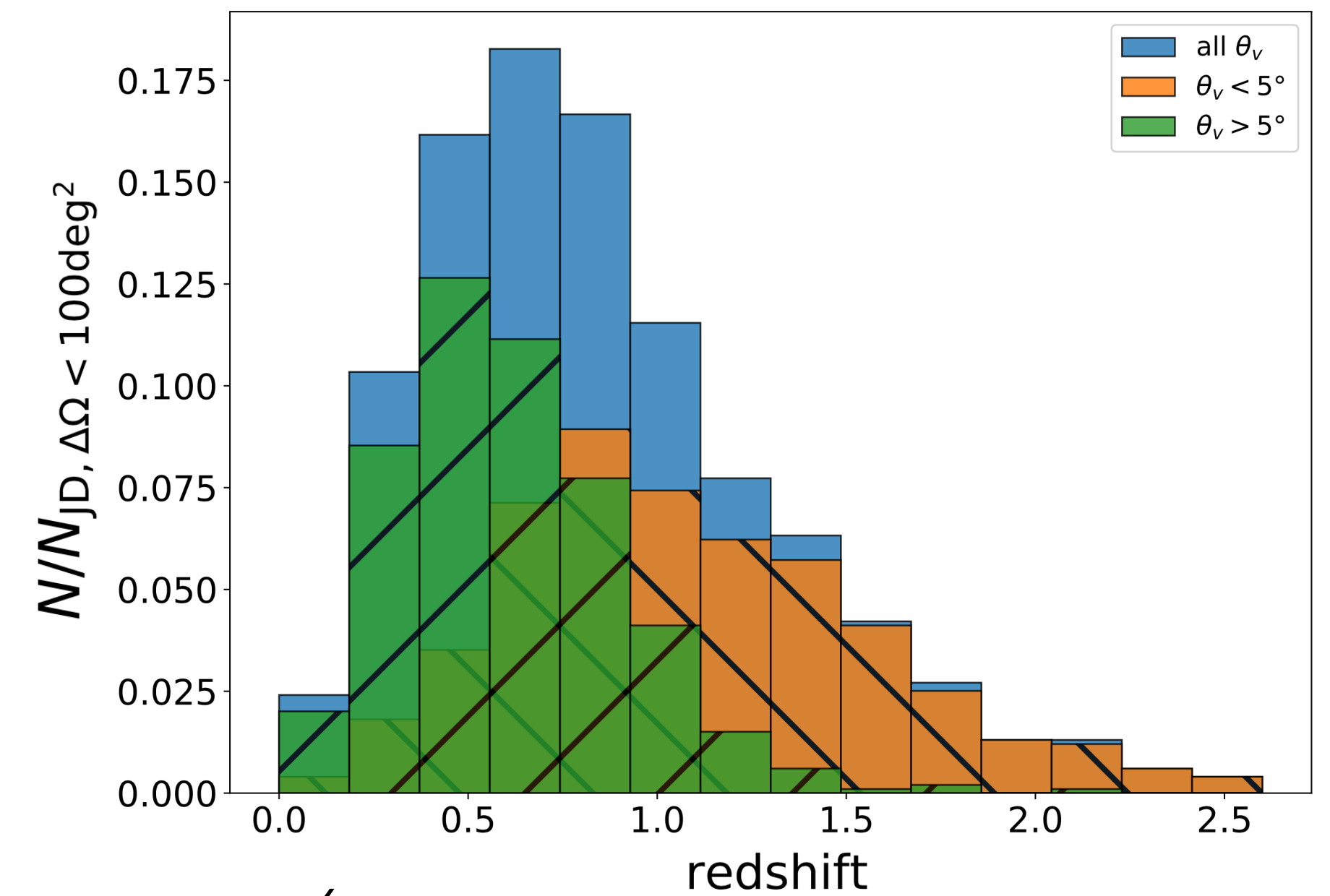
The importance of WFX-ray telescopes

Joint γ -ray+GW

detection efficiency (ET+Fermi-GBM)



Redshift distribution of joint X-ray+GW detections, in pointing mode



Too off-axis to have a detectable γ -ray emission

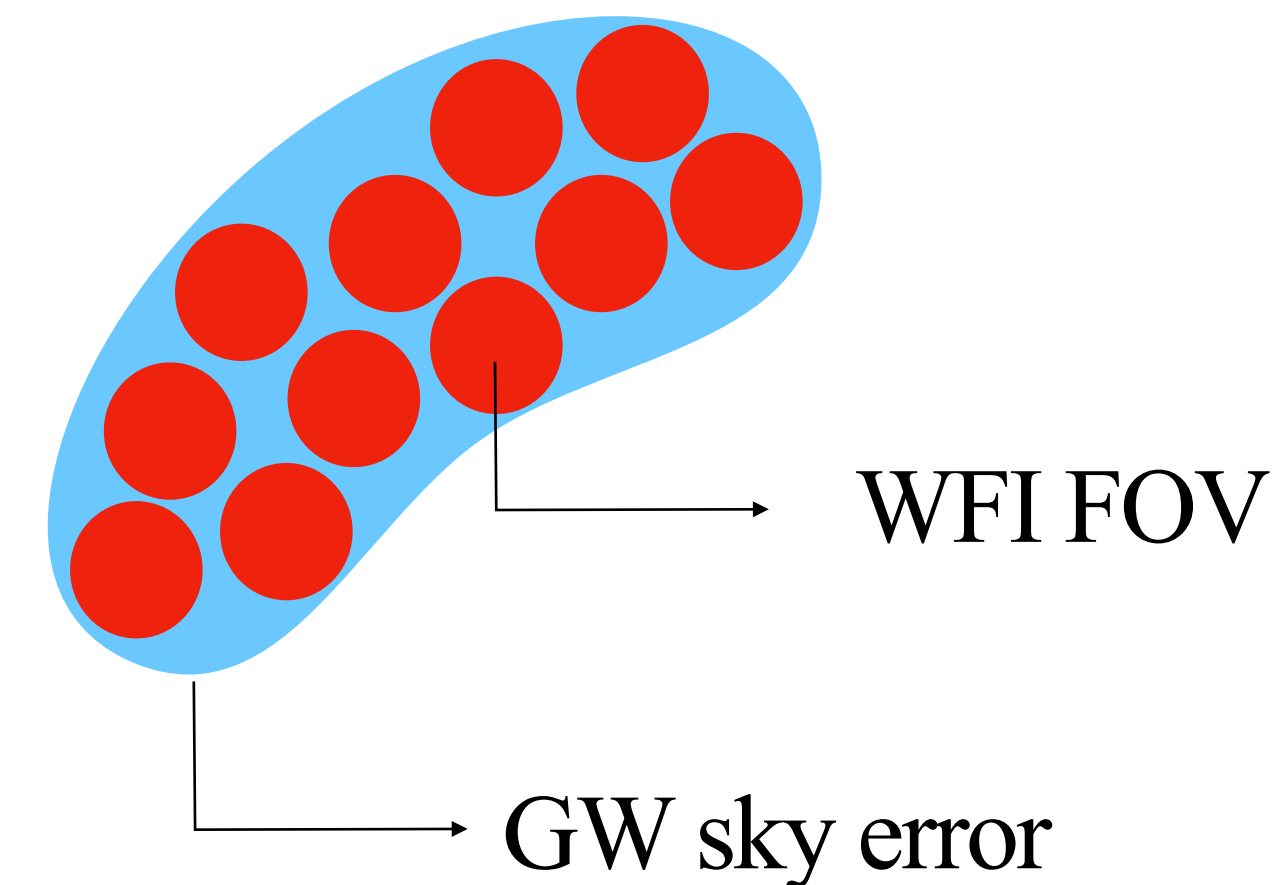
WFX-ray telescopes can significantly **enhance the probability of a joint detection**

The role of sensitive X-ray instruments



1. **X-IFU**: needs arcmin localisation, provided by WFX-ray telescopes
The **totality** of sources identified with WFX-ray monitors can be detected by X-IFU

2. **WFI**: can carry out a **mosaic of a sky region of $\sim 10 \text{ deg}^2$** localisation provided by GW detectors



For ET+2CE

~ 5 joint detections per year,
excluding cases with $\vartheta_v > 50^\circ$

~ 15 joint detections per year,
excluding cases with $\vartheta_v > 30^\circ$

Summary

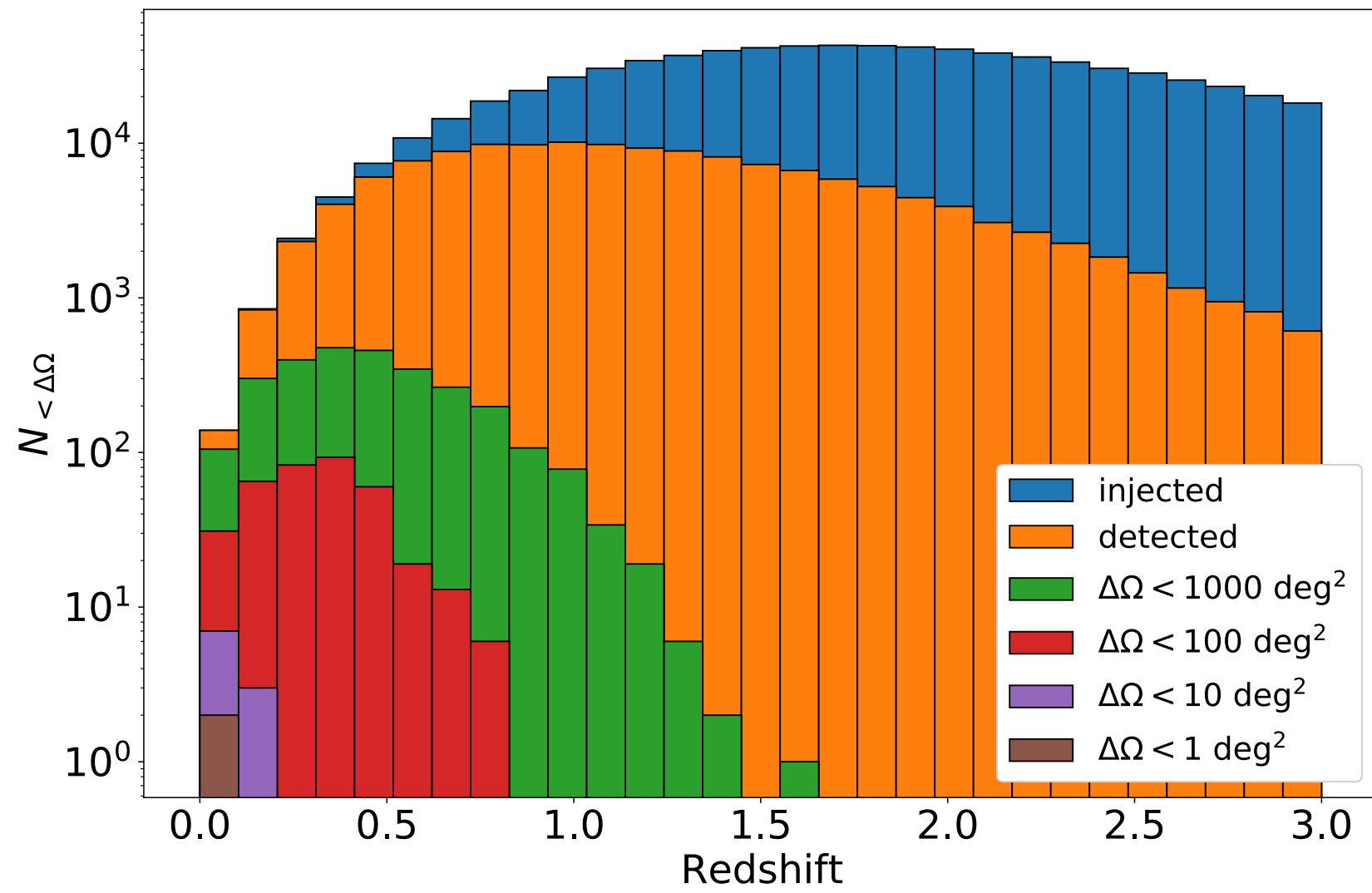
- The remarkable capabilities of next generation GW detectors will allow us to **probe compact binary mergers at cosmological distances**
- The existence of **wide field** X-ray and γ -ray monitors in the next decades will be **crucial**, in order to localise the EM counterpart and possibly the host galaxy with ground-based telescopes
- γ -ray telescopes are ideal to detect sources up to cosmological distances, while **WFX-ray instruments** are optimal for off-axis and sub-luminous events in the local Universe
- Exploiting the **localisation of GW sources** (only with ET or also in synergy with other GW observatories, e.g. Cosmic Explorer) **enhances the probability of having a joint GW+EM detection**
- It is necessary to define an **optimal strategy to select GW events** for which the detection of EM signal is higher

Thank you!

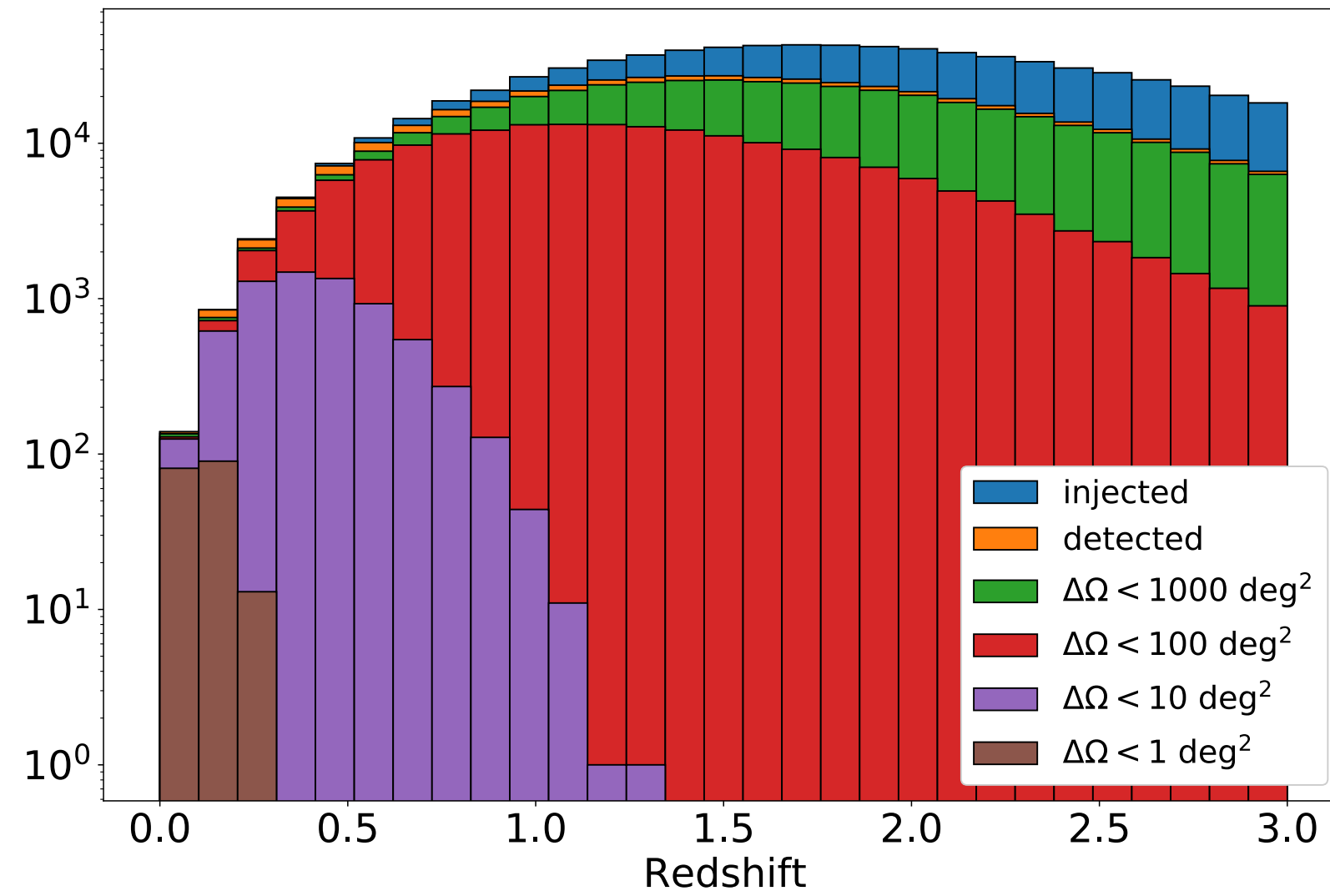
Backup slides

GW sky localisation

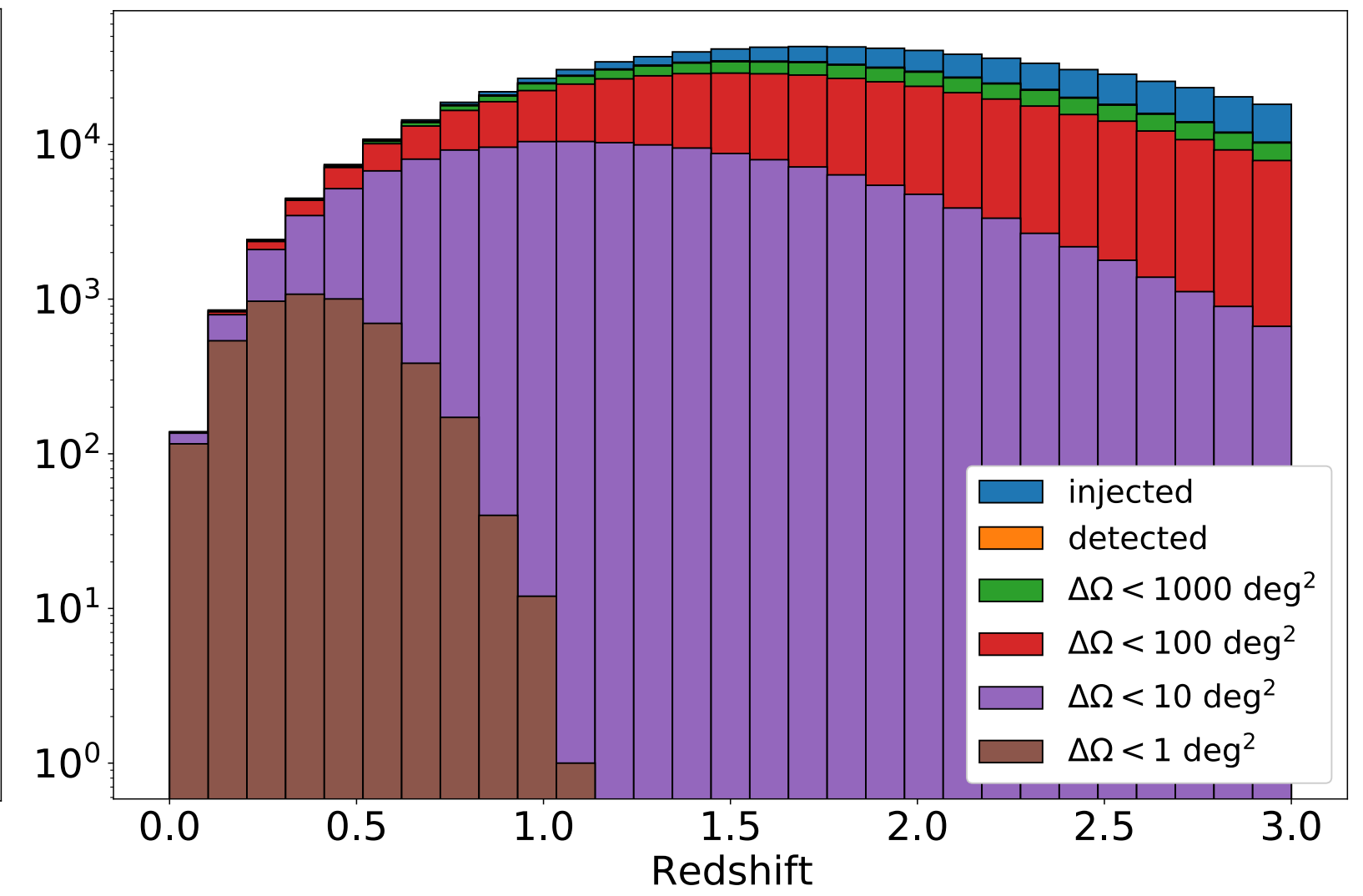
ET



ET+CE



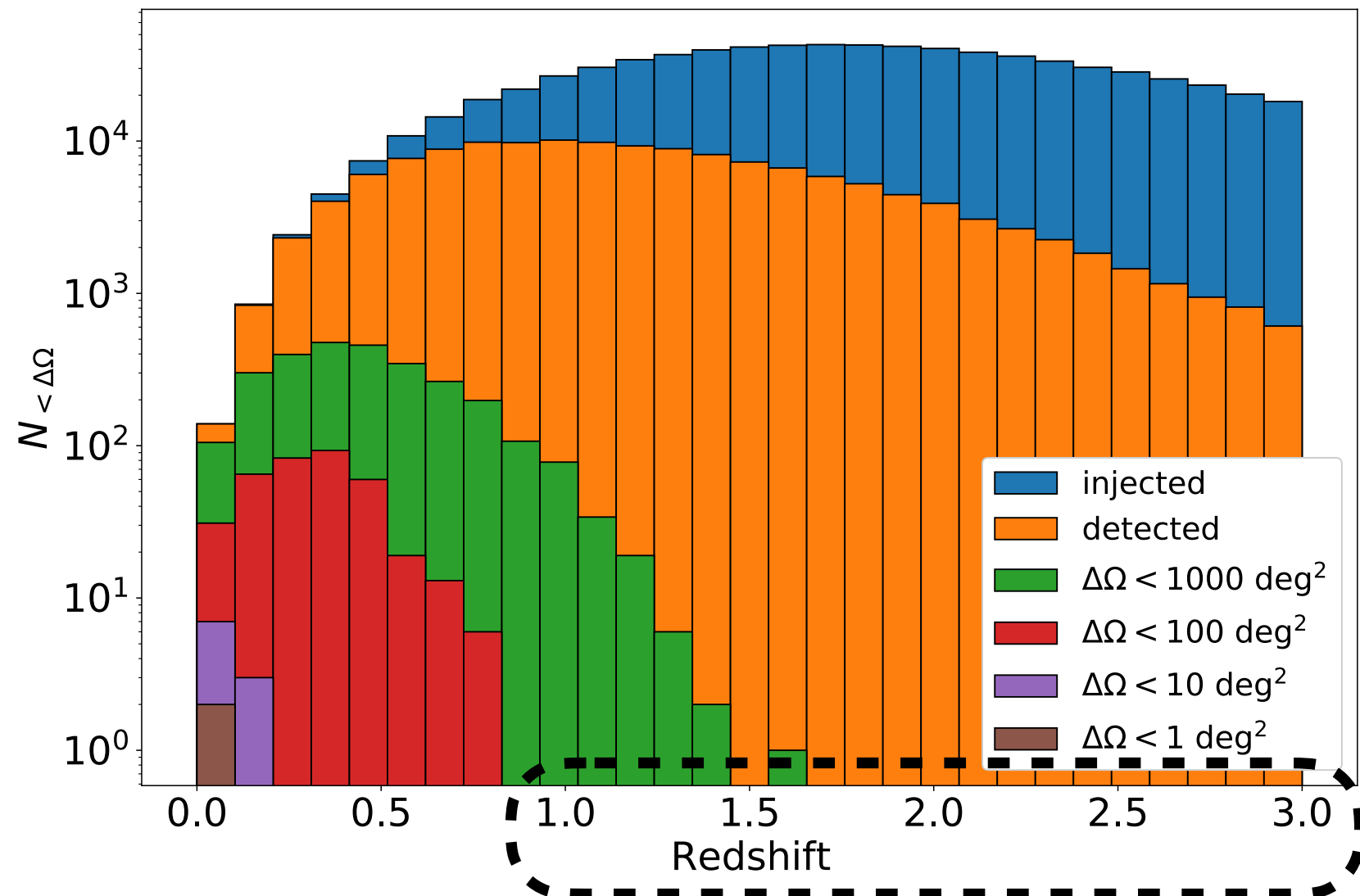
ET+2CE



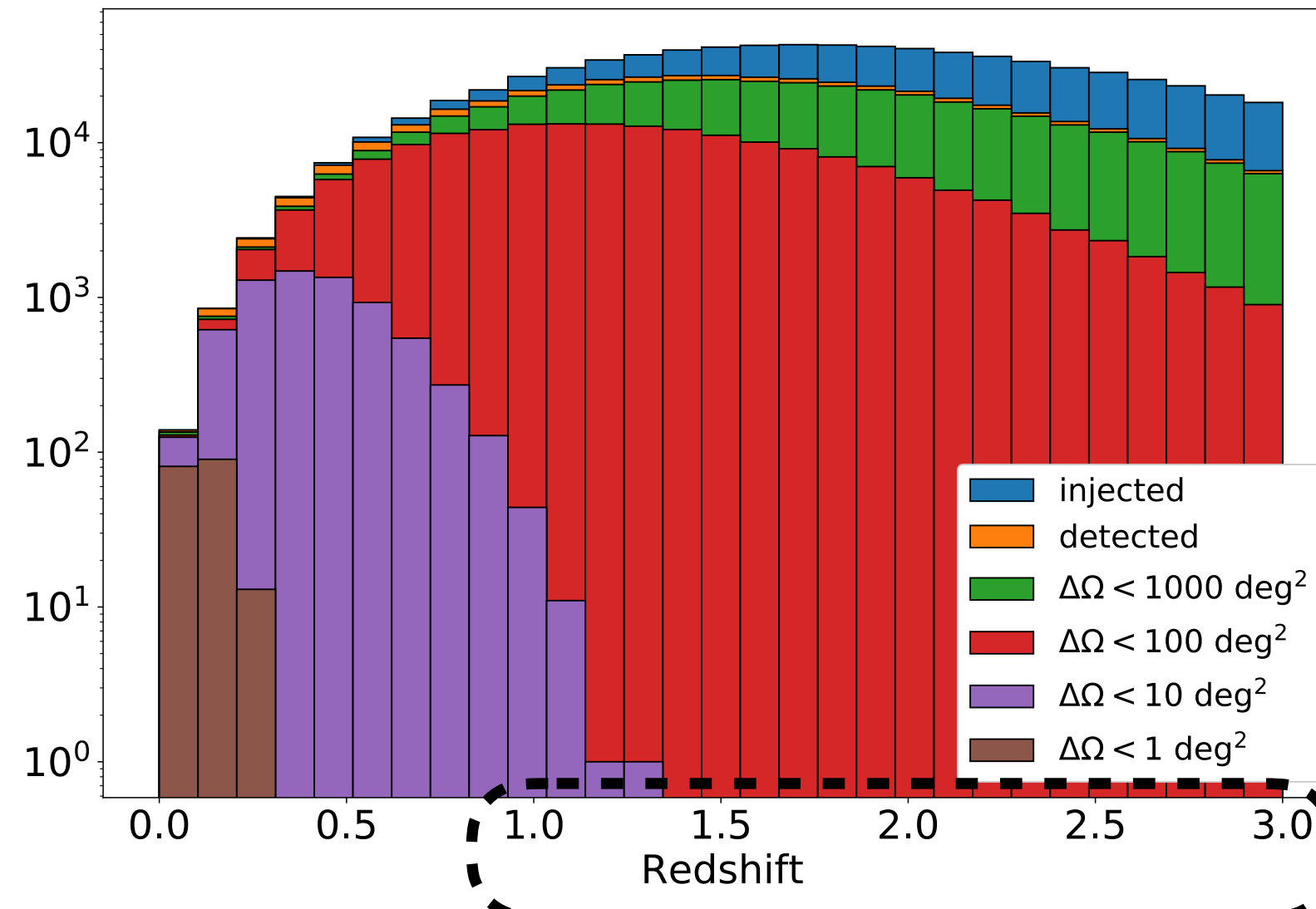
	ET	ET+CE	ET+2CE		ET	ET+CE	ET+2CE
N_{det}	143970	458801	592565				
$N_{\text{det}}(\Delta\Omega < 1 \text{ deg}^2)$	2	184	5009	$N_{\text{det}}(\Delta\Omega < 1 \text{ deg}^2)/N_{\text{det}}$	< 0.1%	< 0.1%	0.8 %
$N_{\text{det}}(\Delta\Omega < 10 \text{ deg}^2)$	10	6797	154167	$N_{\text{det}}(\Delta\Omega < 10 \text{ deg}^2)/N_{\text{det}}$	< 0.1%	2 %	26 %
$N_{\text{det}}(\Delta\Omega < 100 \text{ deg}^2)$	370	192468	493819	$N_{\text{det}}(\Delta\Omega < 100 \text{ deg}^2)/N_{\text{det}}$	0.3 %	42 %	83 %
$N_{\text{det}}(\Delta\Omega < 1000 \text{ deg}^2)$	2791	428484	585317	$N_{\text{det}}(\Delta\Omega < 1000 \text{ deg}^2)/N_{\text{det}}$	2 %	93 %	99 %

GW sky localisation

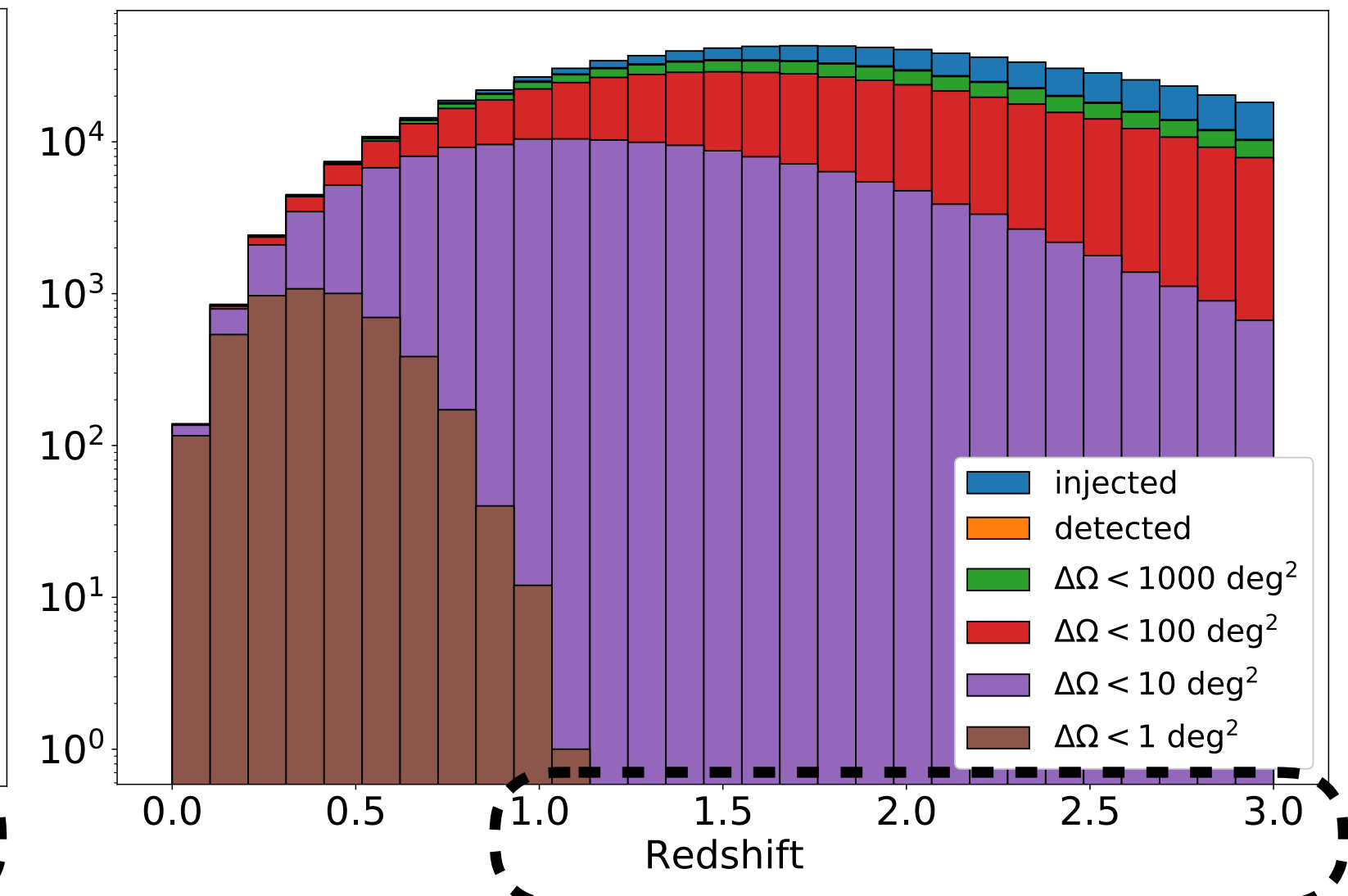
ET



ET+CE



ET+2CE



High- z sources can be well localised only with wide field X-ray and γ -ray telescopes

	ET	ET+CE	ET+2CE		ET	ET+CE	ET+2CE
N_{det}	143970	458801	592565				
$N_{\text{det}}(\Delta\Omega < 1 \text{ deg}^2)$	2	184	5009	$N_{\text{det}}(\Delta\Omega < 1 \text{ deg}^2)/N_{\text{det}}$	< 0.1%	< 0.1%	0.8 %
$N_{\text{det}}(\Delta\Omega < 10 \text{ deg}^2)$	10	6797	154167	$N_{\text{det}}(\Delta\Omega < 10 \text{ deg}^2)/N_{\text{det}}$	< 0.1%	2 %	26 %
$N_{\text{det}}(\Delta\Omega < 100 \text{ deg}^2)$	370	192468	493819	$N_{\text{det}}(\Delta\Omega < 100 \text{ deg}^2)/N_{\text{det}}$	0.3 %	42 %	83 %
$N_{\text{det}}(\Delta\Omega < 1000 \text{ deg}^2)$	2791	428484	585317	$N_{\text{det}}(\Delta\Omega < 1000 \text{ deg}^2)/N_{\text{det}}$	2 %	93 %	99 %